ap

Asian Journal of Physics
Vol. 25, No 3 (2016) 411-445
Available on: www.asianjournalofphysics.in

The solar-stellar connection

Mark S Giampapa
National Solar Observatory, 950 N. Cherry Ave., Tucson, Arizona 85719, USA

A review of some principal results achieved in the area of stellar astrophysics with its origins in solar physics—the Solar-Stellar Connection—is presented from the perspective of an observational astronomer. The historical origins of the Solar-Stellar Connection are discussed followed by a review of key results from observations of stellar cycles analogous to the solar cycle in terms of parameters relevant to dynamo theory. A review of facets of angular momentum evolution and irradiance variations, each of which is determined by emergent, dynamo-generated magnetic fields, is given. Recent considerations of the impacts of stellar magnetic activity on the ambient radiative and energetic particle environment of the habitable zone of exoplanet systems are summarized. Some anticipated directions of the Solar-Stellar Connection in the new era of astronomy as defined by the advent of transformative facilities are presented.

Keywords: Dynamo; Magnetic activity; Cycles; Rotation; Solar- and late-type stars

1 Introduction

The rich array of solar magnetic field-related phenomena occurs not only on stellar counterparts to our Sun but in stars that represent significant departures from the Sun in their fundamental parameters such as mass, gravity and effective temperature. Stellar observations of outer atmospheric phenomena therefore offer environments in which models for magnetic field generation and outer atmospheric heating developed in a solar context can be tested in a parameter space that is unavailable with the Sun alone. Though these phenomena are energetically negligible when compared to the total luminosity of stars (i.e., $\sim 10^{-7} - 10^{-3}$ times the bolometric luminosity), they nevertheless dynamically govern the angular momentum evolution and modulate the radiative and particle output of the Sun and stars. The term 'The Solar-Stellar Connection' has been coined to describe these stellar synergisms with solar physics in the exploration of the generation, emergence and coupling of magnetic fields with the outer atmosphere to produce what we refer to collectively as 'magnetic activity.' The etymology of the term is not known although L. Goldberg attributed its intellectual origins to George Ellery Hale as the guiding principle in Hale's establishment of the solar and stellar facilities at Mt. Wilson Observatory [1].

With the discovery of literally thousands of planets beyond our solar system, the 'Solar-Stellar-Planet Connection' is rapidly emerging as a new and even urgent area of investigation of the impacts of magnetic activity on the structure and evolution of the atmospheres of planets, especially those in the Habitable Zone. In parallel with this rapid development is the advent of transformative facilities for the study of the Sun, our Galaxy and the Universe. In this review, facets of the Solar-Stellar Connection will be discussed both retrospectively and prospectively as we enter a revolutionary, new era for astronomy.

Each topic considered herein is sufficiently extensive in its breadth and depth to be a review paper by itself. Therefore, only selected topics and principal results will be discussed, primarily from an

Corresponding author :
e-mail: giampapa@nso.edu (Mark S Giampapa)

observational perspective. The reader is referred to reviews by: Brun *et al* [2], which also includes a detailed discussion of theoretical advances based on numerical modeling and simulations; Linsky & Schöller [3] on the properties of magnetic fields as observed in non-degenerate stars across the H-R diagram; the predecessor review by Donati & Landstreet [4] on stellar magnetic field detection and its systematic trends with stellar properties in the H-R diagram; Hall [5] with a focus on synoptic ground-based, flux-calibrated observations of particularly Ca II H & K; and, Livingston *et al* [6,7] on the spectroscopic variability of the Sun as a star on solar-cycle time scales.

2 The emergence of the solar-stellar connection

Eberhard and Schwarzschild reported the appearance of a sharp reversal in the K line of singly ionized calcium in photographic plate spectra of the bright red giant Arcturus [8]. The authors noted that the emission occurred "in the middle of the absorption line just as one observes it in a disturbed region of the solar surface." In their spectra of other bright giants, an emission reversal may or may not be present, immediately suggesting that otherwise similar stars can exhibit a range of K line emission. In particular, Eberhard and Schwarzschild detected exceptionally strong K line emission in σ Geminorum while in their sky spectrum, representative of the average Sun, the H and K emission reversal was undetected. These early investigators of the solar-stellar connection concluded "the emission is much stronger in these stars than in the sun." And, further remarking, "Reversals of lines in stellar spectra are not rare. The reversals found here are interesting in that they take place in stars whose spectra are similar to that of the sun and therefore more comprehensible to us." The linkage between stellar chromospheres and the solar chromosphere had been established.

Of course, their "comprehension" was phenomenological in nature: the exact physical mechanism which produces non-radiative heating that, in turn, gives rise to a temperature reversal and the chromospheres (and coronae) in the Sun and stars remains elusive. Nevertheless, from the spatial association between sites of chromospheric H and K emission and magnetic field regions on the Sun [9] it is widely inferred that the ultimate origin of chromospheres and coronae is intimately related to the dissipation of stored magnetic energy. During the 1970s, with the advent of supercomputers and sophisticated non-LTE radiative transfer codes [10,11], the Boulder group led by J L Linsky initiated semi-empirical modeling efforts to extend chromospheric studies beyond the phenomenological by searching for systematic trends in average solar-stellar model chromospheric structure. E Avrett and collaborators at the Harvard-Smithsonian Center for Astrophysics carried out parallel semi-empirical modeling efforts based on the non-LTE PANDORA code [12]. Without reviewing this work in detail, the essential result of these efforts is the finding that the fundamental difference between so-called "active" and "quiet" stars in their mean chromospheric properties is that active stars have higher pressures, manifested as greater mass column densities (g cm^{-2}) at a given temperature, in their chromospheres compared to quiet chromosphere stars [e.g., 13, 14, 15].

As the quality of spectra in resolution and attainable signal-to-noise improved, so did new insights on chromospheric emission in stars that extended beyond its origin. Distance determination is the crucial first step in measuring the fundamental physical properties of stars. Astronomers added another method to their toolbox for estimating stellar distances when Olin C Wilson and M K Vainu Bappu announced in 1957 the discovery of an empirical correlation between the width of the K line emission core and the absolute visual luminosity of a late-type star [17]. This width-luminosity relation, known as 'The Wilson-Bappu Effect,' has been widely applied though its origin remained mysterious for over 20 years after its discovery. But, in 1979, Ayres [18] demonstrated that a correlation between the width of the K line core emission, which is identified with the full-width at half-maximum [17, 19], and stellar surface gravity and, hence luminosity, arises naturally through a consideration of chromospheric line formation processes.

The other critical component of the solar-stellar connection, as with the Sun, is programs in the time domain. The observation of the solar cycle at high precisions with modern instrumentation is only about four decades old. In fact, the discovery of subtle variations in the luminous output of the Sun at the level of 0.1%, and the direct correlation of these brightness changes with the solar cycle of magnetic activity, is a few decades old [20]. Thus, our knowledge of the full range of solar variability that may occur is extremely limited. Given that individual solar cycles are different in form, amplitude and length, and because accurate solar data have been available only for the most recent cycles, there is no direct way of understanding solar variability on the longest relevant time scales.

The observation of solar-type stars, however, can be productively utilized to overcome the temporal confines of the solar database, thereby revealing the potential range and nature of solar variability over time scales that are simply not accessible to the modern solar database of only a few decades. Presciently, Eberhard and Schwarzshild [8] had stated, "It remains to be shown whether the emission lines of the star have a possible variation in intensity analogous to the sun-spot period." Fifty-three years later, Olin Wilson noted in this regard that, despite the accumulation of a large body of data over more than two centuries, an understanding of the solar cycle has been impeded in part because the data refer only "…to a single star with a fixed set of parameters such as age, mass, and surface temperature. It is a reasonable supposition that if analogous cycles could be detected in other stars with different values of the fundamental stellar parameters, the results would be of considerable value in sharpening the theoretical attack on the whole problem" [21]. With this in mind we will discuss in the following aspects of "the attack on the whole problem."

3 Stellar activity cycles

Olin Wilson embarked on a long-term program in March 1966 using the coudé scanner on the Mt. Wilson 100-inch (2.5-m) telescope [21], culminating with his final report covering 11 years of observations of 91 F – M dwarf stars in the solar neighborhood [22]. Wilson's program was undertaken to answer his question, "Does the chromospheric activity of main-sequence stars vary with time and, if so, how?" [22]. Following Olin Wilson's retirement, Sallie L. Baliunas and a host of colleagues continued the Mt. Wilson HK survey but with greater observational intensity. In so doing, rotation periods could be deduced from the short-term modulation of the H and K lines as rotation carried active region complexes across the disk. Due to a lack of funding, the Mt. Wilson HK program terminated in about 2003. Baliunas and collaborators give a summary of results in a paper dedicated to Olin Wilson and with the same title as his landmark 1978 paper [23]. Intermediate results and other discussion are given in [24-28].

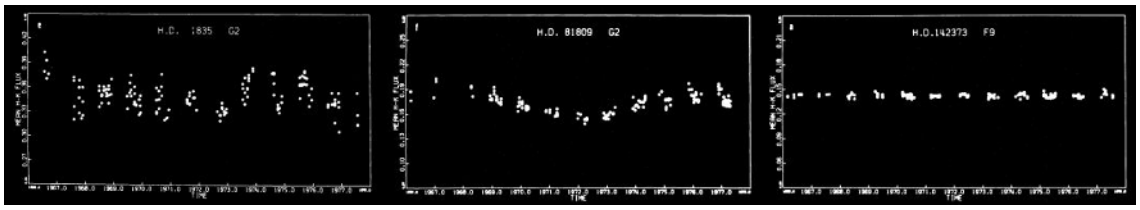

Fig 1. Representative examples of long-term modulation of the Ca II resonance lines from the Mt. Wilson HK Survey program. The left panel is an active star that displays irregular-to-quasi-periodic variability with significant scatter as found in about 25% of the Mt. Wilson stars. The middle panel shows regular variability similar to the solar cycle as seen in ~ 60% of the survey stars. The right panel shows essentially constant Ca II core emission, which is observed in about 15% of the sample. Figure courtesy of J Hall (Lowell Observatory).

The general properties of stellar cycles are encapsulated in Fig 1. We see that about 60% of the Mt. Wilson HK sample exhibits clear periodic variations in the relative HK strength, analogous to that of the solar

cycle. About 25% display irregular variability or quasi-periodic variability that is episodic while 15% of the sample is essentially constant, i.e., flat or perhaps with a long-term trend that may indicate a cycle length in excess of ~ 20+ years.

Those stars with relatively higher mean levels of combined HK emission are characterized by more rapid rotation and only rarely exhibit smooth cyclic variation. Solar-type stars with moderate levels of activity and intermediate rotation periods occasionally show smooth cycles. Stars with HK properties similar to the Sun with solar-like rotation periods display regular, smooth cycles as seen on a seasonally averaged basis [23]. In some stars more than one cycle has been detected—a primary cycle and a shorter, secondary cycle of lower amplitude. For example, HD 190406 exhibits a long-term primary cycle of 16.9 years and a secondary cycle of 2.6 years. The latter was recovered by the Lowell Observatory program, which included an extension of monitoring of some Mt. Wilson program stars [5]. There is evidence of a ~ 2-year cycle in the Sun that may be a secondary cycle to the primary 11-year sunspot cycle [29] though multiple cycle periods do not seem to be a general result in the Mt. Wilson data-set.

Prior to the Mt Wilson H K program summary paper [23], S Baliunas and R Jastrow presented a statistical analysis of a subset of the Mt Wilson sample to infer the distribution of the mean level of chromospheric activity in ostensibly sun-like stars and, as a principal result, an inference of the fraction of stars that were in a Maunder minimum phase [30]. The latter is interpreted as stars with unusually low levels of H K activity (less than that at solar minimum) and flat activity cycles. These objects, of which there were only four (including a metal-deficient K0 star) within a total sample of only 13 solar analogs, were utilized to estimate the time the Sun could be in this exceptionally quiescent phase of otherwise normal cyclic variation. These investigators found a bimodal frequency distribution of magnetic activity with approximately one-third of the solar-type stars in a presumed Maunder minimum, implying that this could be the frequency the Sun enters Maunder minima, with implications for impacts on global climate. However, Wright [31] determined on the basis of *Hipparcos* parallaxes that the exceptionally quiescent stars in the Baliunas & Jastrow subsample were, in fact, evolved stars that exhibited low levels of activity as a consequence of their age.

The initial claims in Baliunas and Jastrow [30] illustrate the critical importance of knowing the evolutionary status of a star before concluding that it is a solar analog in addition to the need for having a statistically reliable sample [32, 54]. In comparison, Giampapa *et al* [33] found that only 17% of a homogeneous sample of solar analogs exhibited HK index values less than that at solar minimum. The distribution of HK index in Giampapa *et al* [33] also is unimodal, which is interpreted to mean that exceptional quiescence is a low-amplitude extension of a solar-like dynamo rather than a separate dynamo mode. Interestingly, Hall and Lockwood [34] also found a unimodal distribution of H and K emission levels in a sample of field solar-type stars. In addition, they identified a subsample of noncyclic, flat stars. These objects exhibit HK levels that span the range from below solar minimum to in excess of solar maximum, thus indicating that a flat time series of HK measurements is not necessarily a consequence of relatively reduced magnetic activity.

In a recent analysis of published Mt. Wilson HK Survey data, Choi *et al* [35] cull from the 111 stars observed 23 G dwarf stars and reanalyzed their cycle lengths. These investigators utilized various age indicators to divide their sample between solar-age stars and young solar-type stars, and examined the correlation between normalized chromospheric emission and stellar activity cycle length. Choi *et al* [35] find that mean chromospheric emission and cycle length are correlated with a clear segregation between young and old stars in the slope of their respective relations. This relation may be a manifestation of the empirical correlation of rotation and activity combined with a correlation between rotation rate and cycle period, as we will discuss in the next section.

4 Dynamo-related properties of solar-type stars

Early work found that Ca II emission is directly related to rotation and appeared to decline with age [36-38]. With the advent of the *Einstein* satellite observatory and its extensive stellar X-ray observations, Pallavicini *et al* [39] determined an initial empirical form of the rotation—activity relation, i.e., (approximately) $L_x \sim (v \sin i)^2$. Relationships such as these were emphatic confirmation of the dynamo-origin of activity and, in the case of coronal emission, its magnetic field-related origin, especially in view of the fact that there is no significant photospheric contribution to the emission from cool stars at soft X-ray wavelengths.

The advent of the *ROSAT* mission with its all-sky survey and the *Chandra* Great Observatory significantly added to the available stellar X-ray data, enabling Pizzolato *et al* to expand on the early work based on *Einstein* [40]. These investigators confirmed the correlation of X-ray luminosity with rotation for periods greater than ~ 2 – 3 days. At shorter rotation periods, the coronal X-ray emission appears to saturate at a level of log $L_x \sim 30$ erg s^{-1} or log ($L_x / L_{\rm bol}$) ~ –3.2 with the onset of a possible decline at rotation periods shorter than about 0.4 days. When examined according to bins in stellar mass, each bin exhibits an increase in normalized X-ray emission with shorter rotation period, eventually reaching a maximum, or saturation level at about ~ -3 in log ($L_x / L_{\rm bol}$) though more near ~ – 4 in the F5 V – G0 V regime [40]. The latter may indicate a reduced efficiency in magnetic flux production that leads to X-ray emission in stars with rapid rotation but thin convection zones. The onset of the saturation phenomenon occurs at longer rotation periods toward lower masses and greater fractional convection zone depths. For example, for solar-mass stars saturation begins at a rotation period of about 2 days while for red dwarfs X-ray emission saturates at rotation periods ~ 10 days. Given the decline in radius toward cool stars, this would suggest that enhanced activity occurs at relatively lower rotational velocities, thus suggesting more efficient dynamo field generation in stars with thick convection zones. The form of the linear relation between rotation period and $L_x / L_{\rm bol}$ (or L_x) following the saturation regime is independent of fractional convection zone depth.

The role of differential rotation is less clear. In an analysis of over 40,000 stars in the *Kepler* data base selected according to range of photometric variation, Reinhold *et al* [41] find that the absolute shear ($\Delta\Omega$) exhibited only a slight increase in the effective temperature range of 3500 K – 6000 K and a steep increase in the F dwarf region above 7000 K. Thus, differential rotation would seem to play little role in the form of the rotation-activity relation. However, this analysis is biased toward relatively higher activity levels, which is understandable since this is where spot modulation of the photometric light curve, and subtle period changes interpreted as the signature of differential rotation, are most evident.

Giampapa [42] reviews empirical relationships between rotation and cycle properties that have been ascertained from the Mt. Wilson HK program. In general, cycle frequency increases with rotation frequency as $\omega_{\rm cyc} \sim \Omega^{1.6}$. The form of this correlation is actually very similar to that of the normalized differential rotation versus inverse Rossby number, leading Saar [43] to suggest that differential rotation has left an imprint on cycle periods and their relationship to rotation. Sarr [44] find a relationship between cycle amplitude and cycle frequency (normalized by rotation frequency) in the form of two branches that they refer to as the "Inactive" or "I" branch and the "Active" or "A" branch. Both branches are log-linear with the *A* branch somewhat steeper than the *I* branch. The Sun lies within the scatter of the fit to the *I* branch. The transition between these branches may indicate that the dynamo is partly unstable [45].

By contrast, Böhm-Vitense [46] provides an additional perspective on the cycle period – rotation period relationship as seen in Fig 2. Here we see the "Active" and "Inactive" branches, this time in a graph of cycle period versus rotation period. The secondary cycles are designated by triangles and correspond to mainly stars on the "Active" branch. The secondary cycles are on the extrapolation of the *I* sequence to faster rotation periods. Böhm-Vitense [46] therefore suggests that the operative dynamo for the *I*-sequence stars must also be operating in the *A*-branch stars and that the secondary cycles arise from the same *I*-branch

dynamo mechanism. Note that they also have rotation periods faster than solar. The diagram suggests that in stars with detectable cycles and rotation periods that cycle period increases with rotation period more sharply on the *A* branch than the *I* branch. A possible interpretation of Fig 2 is that it is a manifestation of two dynamos that operate on a different number of rotations per cycle. We note that the Sun as seen in this diagram appears between the two branches giving the impression that it is a "transition object." Perhaps so, but we would caution that in this sample the "Inactive" branch stars—shown here as asterisks—are all K dwarf stars with slower rotation periods than the Sun. These cooler stars also define the range of the *I* branch in this diagram. Therefore, this may not be a suitable sample for comparison with the Sun and emphasizes the importance of knowing how a stellar sample is defined before we can draw conclusions comparing the behavior of the Sun with that of other stars. On the other hand, the K dwarfs on the *I* branch do represent a mode of dynamo operation in the limits of slow rotation and relatively thicker convection zones than the Sun.

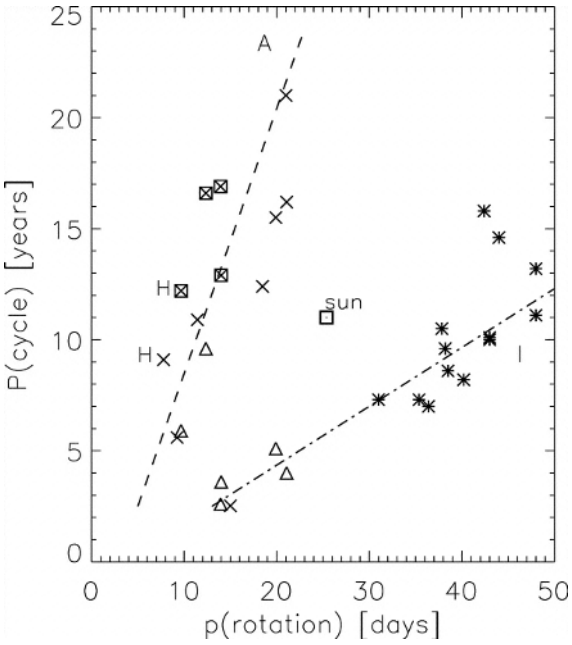

Fig 2. Activity cycle periods, P_{cyc} (years) as a function of rotation period, p_{rot} (days). The data follow two sequences, the relatively young, active A sequence (*dashed line*) and the generally older, less active I sequence (*dash-dotted line*). The letter H denotes Hyades group stars, crosses represent stars on the A sequence, and asterisks indicate stars on the I sequence. Squares around the crosses are stars with $B - V < 0.62$. Triangles show secondary periods for some stars on the A sequence. The Sun is indicated (from [46]).

The existence of branches delineated by activity in rotation—cycle period diagrams is reminiscent of the so-called Vaughan—Preston Gap [47] that is seen in a diagram of normalized Ca II chromospheric emission strength vs. color (Fig 3). A distinctive gap is apparent between active and younger stars, and more quiescent stars, similar to the Sun. Assuming no discontinuity in the local star formation rate, this diagram may be a manifestation of either different dynamos operating in active and inactive stars or two modes of the same dynamo that undergoes a transition at a critical rotation rate or Rossby number, corresponding to transitions between the Active and Inactive branches discussed previously. In particular, Brandenburg *et al*

[48] find a similar gap or jump in their diagram of cycle frequency (normalized by rotation frequency) vs. mean HK emission at log $R'_{HK} \approx -4.75$, which is where the gap appears in Fig 3 for solar-type stars with colors later than $(B - V) \sim 0.6$. The origin of this segregation between active and inactive is unclear though instabilities related to the α-effect (i.e., the regeneration of poloidal field) in kinematic α-ω dynamos may be relevant [49, 48]. Given the correlation of Ca II emission strength with magnetic fields, the gap in Fig 3 suggests that there is a critical threshold in magnetic flux that distinguishes between chromospherically active and quiescent stars.

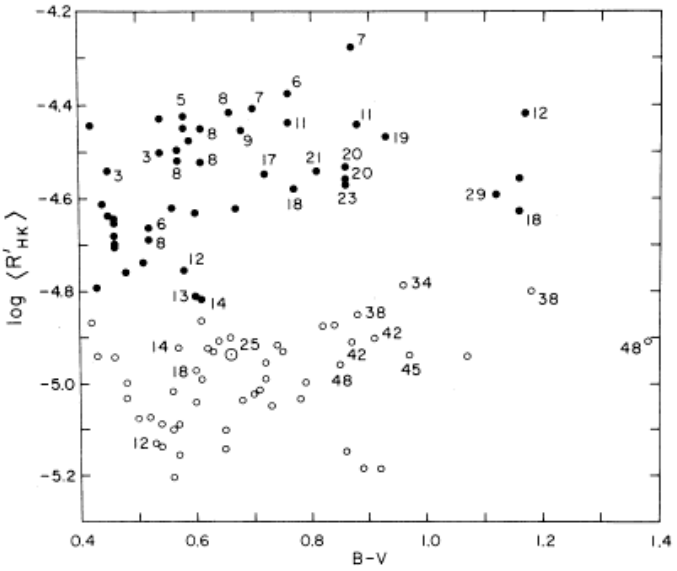

Fig 3. Mean normalized chromospheric emission as a function of color [26]. The numerical labels are rotation periods in days. The location of the mean Sun is indicated. Filled circles represent ostensibly younger stars and open circles denote stars considered to be relatively older.

4.1. Rotational evolution in main-sequence solar-type stars

A significant consequence of magnetic field generation by regenerative dynamo action is angular momentum evolution through rotational decay on the main sequence. Emergent magnetic fields and associated mechanical heating give rise to stellar coronae and winds (e.g., see [50] and references therein for the evolution of thought, both intellectually and professionally, in the context of this topic). The coupling of the stellar wind with the field exerts a torque that acts to spin down the star, at least as observed in the rotation of its outer layers [51, 52, 2]. On the basis of measured projected rotational velocities in members of a sequence of open clusters of known age, Skumanich [36] empirically determined that the time dependence of the rotation, as well as chromospheric activity and lithium depletion, was proportional to $t^{-1/2}$. Though alternative forms have been proposed [53], and despite the fact that the original data used by A. Skumanich were sparse, the "Skumanich law" has proven remarkably robust. However, intriguing departures recently have been identified at solar age or older [54, 55]. We anticipate that the current *K2* mission will disclose more such objects.

The investigation of open clusters has revealed that rotational decay and the associated chromospheric emission is mass dependent. In Fig 4 from [56] the distribution of rotational velocities as a function of color is shown in the young Pleiades open cluster and the older Hyades cluster.

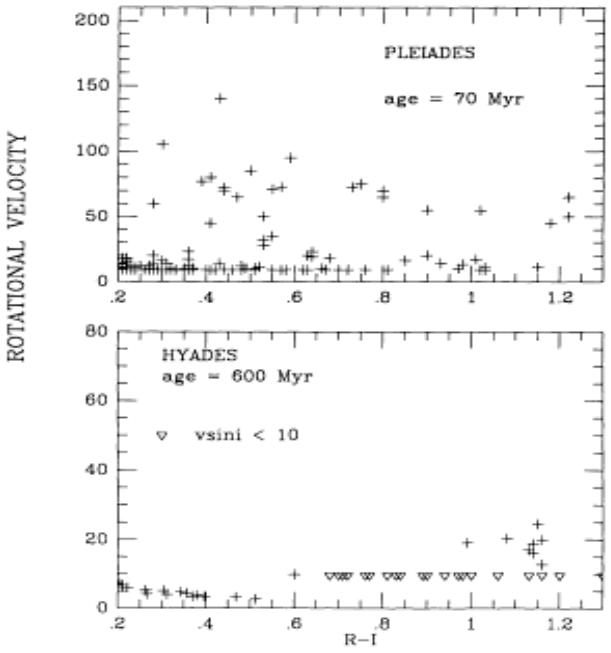

Fig 4. Projected rotational velocities as a function of spectral type as represented by ($R - I$) color in the young Pleiades cluster and the comparatively older Hyades from [56]. For reference, a G2 dwarf has a ($R - I$) color of 0.33 while ($R - I$) = 1.19 for a dwarf M2 star. Note the difference in scale for the ordinate (units: km s^{-1}) in each panel.

Inspection of Fig 4 reveals that rapid rotation exceeding ~ 50 km s^{-1} is present in the Pleiades from late F through early M spectral types. By the age of the Hyades, however, stars have spun down to rotational velocities less than 10 km s^{-1} (the upper limit of the measurements) though a population of rapidly rotating late K – dwarf M stars remains. Let us examine the possible origins of this mass dependence in the change in angular momentum associated with rotational spin down. In general terms we have

$$\dot{J} = \Omega \dot{I} + I\dot{\Omega} \tag{1}$$

where J is angular momentum, Ω is stellar angular velocity and I is the moment of inertia. We neglect the first term since it is important only for stellar evolution time scales. That is, for stars on the ZAMS we have $\dot{I} \approx 0$. Following Mestel [57] and Kawaler [58] we have for magnetized winds

$$\dot{J} = \frac{2}{3}\dot{M}R^2\,\Omega\left(\frac{r_A}{R}\right)^m \tag{2}$$

where $\dot{M}$ is the mass loss rate due to winds, R is the stellar radius, r_A is the radius of the Alfvén point and m = 1 for a dipole field and 2 for a radial field. The ratio r_A/R is determined by the field strength and the power m is determined by the field geometry. Combining and rewriting the above relations in terms of the relative change in rotation period and the moment of inertia yields

$$\frac{\dot{P}}{P} \sim \rho^{1/2}\,\frac{B_s}{K}\,\frac{R^2}{M}\left(\frac{r_A}{R}\right)^{m'} \tag{3}$$

where we used that the Alfvén speed is the wind speed at the Alfvén surface; mass continuity; and, a scaling of the decline of the surface magnetic field strength with distance out to the co-rotation radius. In the above K is

the leading constant for the moment of inertia. Assuming similar wind densities and magnetic topologies we can compare the relative rotational period changes in a low mass M8 dwarf to a solar-like star. In particular, we compare the ratio B_sR^2/M with the surface field strength, $B_s \sim 3000$ G for the dM8 star and 1500 G for the sun-like star, respectively. With $R \sim 0.1R_\odot$ and $M \sim 0.1M_\odot$ for the late M dwarf the aforementioned ratio is ~ 0.2, implying slower spin-down relative to solar-type stars, which is what we observe. But by mid-M spectral types this ratio is ~ 0.6, i.e., closer to the estimate for solar-type stars suggesting that this alone cannot be the whole explanation for the trend of slower spin-down with mass over a factor ~ 10 in age. Magnetic topology and its possible variation with stellar parameters must play an important role. An abrupt change in large-scale magnetic topologies at ~ M3 coincides with a rapid change in the size of the radiative core [59, also see 60]. Donati *et al* [59] suggest that this change in topology could be the source of the reduced efficiency of magnetic braking in low mass dwarfs. A contrasting view, where the dominant factors are the rapid change in mass and radius across the fully convective boundary irrespective of field geometry, is given in Reiners and Mohanty [61].

Another aspect to consider is the variation of moment of inertia with spectral type on the main sequence. This is relevant to the question of what is actually spinning down—the whole star or just the outer convection zone? We display in Fig 5 the distribution of stellar rotation periods with $(B - V)$ color in the young open cluster, M35, from [62].

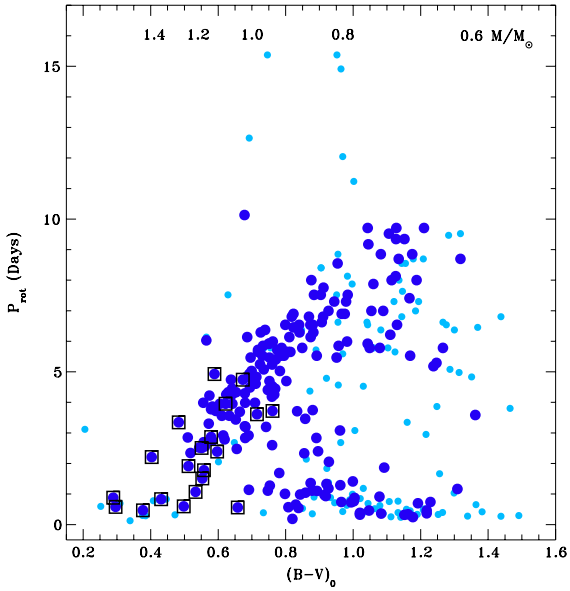

Fig 5. The distribution of rotation period with color in the young M35 open cluster (age ~ 150 Myr) from [62]. A corresponding mass scale is given at the top. The symbol colors represent the method used to determine membership. Two sequences are evident with slower rotators comprising the upper diagonal I-sequence and fast rotators in the lower horizontal C-sequence along with an apparent gap between the two sequences.

Barnes [63] proposed that this diagram consists of two sequences: the "I (Interface) Sequence" where the radiative core and outer convective envelope are coupled and the "C (Convective) Sequence" with decoupled radiative and convective cores. The evolution of surface rotation rates for stars on the *C* sequence is governed by moments of inertia of the convective envelope and inefficient wind-driven loss of

angular momentum linked to small-scale magnetic fields. On the I-sequence, large-scale (solar-like) magnetic fields from an interface dynamo couple the core and envelope. The rotational evolution on the I sequence is governed by the moment of inertia of the entire star and more efficient angular momentum loss. In this scenario rotational evolution begins on the C sequence and evolves onto the *I* sequence when rotational shear between the stellar core and the envelope establish a large-scale dynamo field that couples the two zones and provides efficient magnetic wind loss.

From the apparent gap between the I and C sequences we infer that any coupling or decoupling occurs on short time scales that are much less than the cluster age of about 150 Myr. From helioseismology we find that the internal rotation at mid-latitudes is already close to that at the base of the convection zone in the tachochline. If there were an earlier "decoupling" then it would have to "recouple" somehow. In addition, the Alfvén crossing time of the star is short compared to rotational evolution time scales, even for very modest internal magnetic fields, suggesting that a decoupled spin down of the outer layers alone is not physical. There is a further aspect of this view that must be considered. The relative change in rotation period in terms of moment of inertia is given by

$$\frac{\dot{P}}{P} \propto \mathrm{M}\,\frac{R^2}{I}\left(\frac{r_A}{R}\right)^m \tag{4}$$

where I is the moment of inertia of either the star or the outer convection zone. The model calculations by Barnes and Kim [64] reveal a rather flat trend in the moment of inertia of the convection zone from $(B-V) \sim 0.7 - 1.4$ suggesting no mass-dependence in the rotational decay if moment of inertia of the convection zone is the principal factor. In this case, other factors in the above equation become more important in governing spin down and its mass dependence where low mass stars spin down more slowly than higher mass, solar-type stars.

5 Brightness variations in solar-type stars

A notable discovery of 20$^{\text{th}}$ century solar physics is that both the total and spectral irradiance of the Sun are variable on long and short time scales. In particular, the total solar irradiance varies directly with the solar magnetic flux cycle of the Sun in the sense that it is about 0.1% brighter at sunspot maximum and fainter at solar minimum. Short-term total irradiance variations are primarily governed by the disk passage of sunspots and are generally in the range of ~ 0.1% – 0.3%. A comprehensive review of the solar irradiance variability is given by Solanki *et al* [65]. In this section we will summarize the key results that have emerged on analogous, magnetic field-related photometric variability in solar-type stars.

The initiation of a program to investigate the presence and nature of brightness variations on solar-type stars was a natural extension of the Mt. Wilson HK program combined with the discovery of solar irradiance variations that are correlated with magnetic activity. W Lockwood and B Skiff (Lowell Observatory), along with R Radick (Air Force Research Lab/National Solar Observatory), embarked on such a long-term program of ground-based, high precision differential photometry of solar-type stars in the field and in open clusters. Over a decade of photometric monitoring is summarized in [66, 67].

A principal result of this program is that the amplitude of long-term brightness variations in visible (Strömgren) photometric bandpasses is directly correlated with chromospheric activity. This is also true of the annual short-term rms variability though, of course, with considerable scatter in each bin of normalized chromospheric emission with the range of variation increasing with chromospheric activity. The Sun as a star is among the quiescent stars in these observed correlations. A salient result of this effort is displayed in Fig 6 where the short-term and long-term correlations between HK emission, $(B-V)$ color and the nature of the correlation with photometric brightness, are indicated.

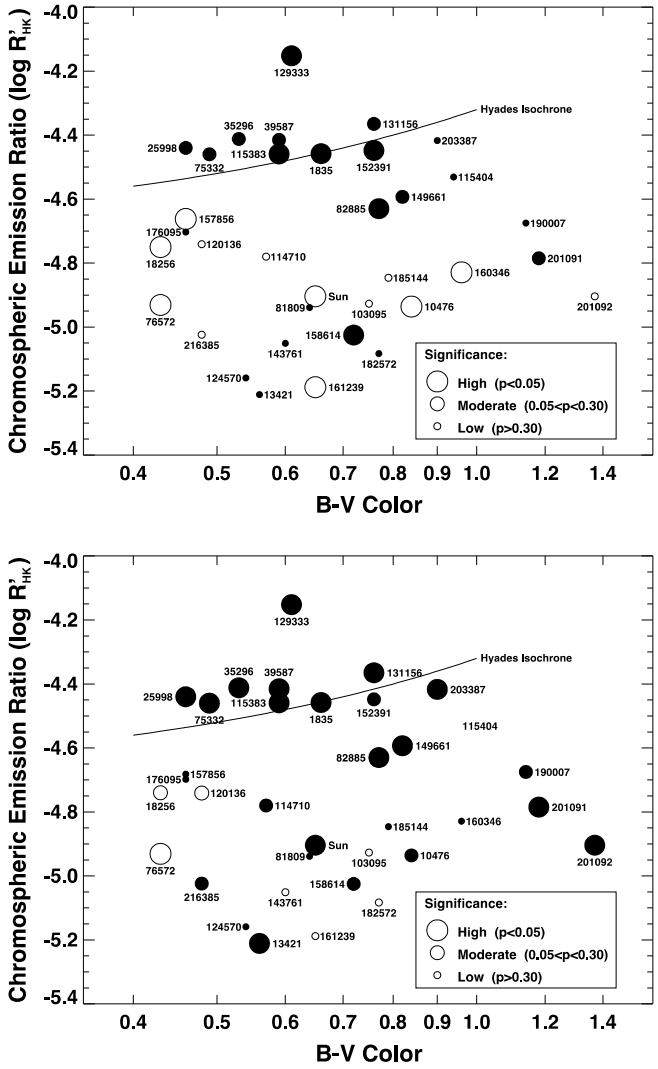

Fig 6. Long-term variations between chromospheric emission and photometric variations in two visible (Strömgren) bands as a function of color (upper panel). The behavior on short time scales is given in the lower panel. The symbol size is proportional to the significance of the correlation while the sense is indicated by filled circles (inverse correlation) and open circles (direct correlation of brightness changes with chromospheric emission). From Ref [67].

In these diagrams anti-correlated behavior, i.e., the star becomes fainter, occurs at relatively high chromospheric emission levels while a direct correlation between the amplitude of brightness changes and chromospheric emission is present in stars with more solar-like levels of chromospheric activity. The Sun appears to share the characteristics of both populations: it exhibits anti-correlated variability on short (rotational) time scales while its photometric variations are directly correlated on long (cycle) time scales. It is interesting, too, that the demarcation between direct and inverse correlation in long-term variations occurs in the range of $R'_{HK} \sim -4.8$ to -4.6, which is where the Vaughan-Preston Gap (Fig 3) also occurs, possibly indicating a change in dynamo mode as discussed in §4.

The morphological origin of this trend is widely considered to be a transition between facular-dominated variations and brightness changes that are spot-dominated in the net effect. That is, at high activity levels the filling factor of dark spots is larger and this leads to a net dimming effect. At solar-like levels the spot filling factor is lower, hence the brightness changes are dominated by the facular contribution.

Interestingly, some objects can exhibit transitions between these dominant modes of correlated brightness-activity variations. For example, Hall *et al* [165] reports that the solar-type star, HD 140538, which is slightly more active than the active Sun, displayed a change from direct activity-brightness variations to inverse variations during the total period of observation from 1997 – 2008. The transition corresponded to a transition from noncycling to cycling behavior. Its mean normalized chromospheric HK emission of $\log R'_{HK} = -4.80$ or about 1.4 times more active than the average Sun, suggests that this level of activity marks the transition from facular to spot dominance in overall brightness variations. Inspection of Fig 3 reveals that this value of R'_{HK} also marks the onset of the Vaughan-Preston Gap.

The *Kepler* mission has expanded on these results with its exquisite photometry in the visible 400 nm – 900 nm broadband. In particular, emerging results from F. Bastien and her collaborators confirm the correlation of increasing range of photometric variation with higher mean levels of Ca II H and K chromospheric emission as found earlier by Lockwood *et al* [66] but now for a much enlarged sample of field stars. The *Kepler* and ground-based data suggest that the Sun is at a boundary between a band of stars with enhanced chromospheric emission and larger amplitudes of photometric variability, and those with a relatively smaller range in brightness variations and quiescent HK emission. However, the evolutionary status and solar-like nature of the most quiescent objects remain to be confirmed [68].

The nature of solar variability in comparison with that of solar-type stars has been investigated with the expanded sample based on the ultra-high precision photometry available from the archive for the *Kepler* field. Gilliland *et al* [69] determined that 60% of the solar-type stars were more photometrically variable and, hence, more active than the Sun thus raising the paradoxical question of whether the Sun was a solar-type star! However, in a detailed examination of the *Kepler* data reprocessed in a different manner, Basri *et al* [70] find essentially no distinction between the Sun and the variability of solar-type stars in the *Kepler* sample on the time scales that they considered, i.e., ~ 12 hours – 8 days. The results from *Kepler* are consistent with prior studies, notably [67, 166, 165], that found solar photometric variability to be similar to true solar analogs.

In a recent examination of the Sun-as-a-star data-set based on Ca II K line spectra obtained with the SOLIS Integrated Sunlight Spectrometer, and SORCE satellite irradiance data, during the overlapping period of observation from 2006 – 2014, no correlation was seen between the total flux in the visible "*Kepler* band" and the 1 Å K line index [68, 71]. A closer examination of subsets of the data reveals that correlations appear but only on an episodic basis that may be tentatively attributed to the disk passage of active region complexes. Further investigation of the relationship between brightness variations in the visible and chromospheric emission in the Sun as a star is in progress.

In the case of solar-type stars, Giampapa [71] discusses an initial investigation of the relative contributions of spots and faculae in the visible band observed by *Kepler*. Adopting a simple three-component model (spots, faculae and photosphere), variations in the visible are found to be dominated by spots though the possibility of faculae with an enhanced, non-solar contrast is not excluded. Giampapa [71] discusses special cases that may arise in stellar variability where the facular contrast plays a critical role in determining the amplitude of variability in the visible. In a detailed consideration of whether solar brightness variations are faculae- or spot-dominated on multiple time scales, Shapiro *et al* [72] find that brightness variability for the Sun as a star is spot-dominated on rotational time scales. For out-of-ecliptic-viewing, mimicking viewing the Sun as a star at an inclined rotation axis, Shapiro *et al* [72] find that brightness variations are faculae-dominated for inclinations less than $i = 30^{\circ}$. In brief, the apparent facular domination in this case is due to

foreshortening and continuum opacity effects that act to reduce the apparent spot contribution. In conclusion, it is clear that both the facular and spot contributions combined with the effects of viewing angle must be considered in the interpretation of the origins of variability in solar-type stars on multiple time scales.

6 Special cases: the F and M dwarf stars

The main sequence F and M stars merit special consideration because they respectively represent dynamo field generation in the limit of thin and thick convection zones. The onset of solar-like magnetic activity coincides with the appearance of outer convection zones in the dwarf F regime. The transition from partially convective to wholly convective interiors occurs in the M dwarf region of the H-R diagram with fundamental implications for the nature of the dynamo [73].

6.1. F dwarf stars

The dwarf F stars are characterized by rapid rotation and shallow outer convection zones. These stars also have strong chromospheric and coronal emission levels that are typically 10 – 100 times that of the quiet Sun. Despite the high level of presumably magnetic field-related activity, there is a distinct lack of observed surface inhomogeneity as manifested by either no, or very low, modulation of either H or K or the continuum in photometric bands.

Giampapa and Rosner [74] argue that the high angular velocities of these stars lead to the production of smaller flux ropes at the bottom of the thin stellar convection zone. In particular, the calculations by Schmitt and Rosner [75] showed that the spatial scales of generated flux ropes scale as $\Omega^{-1/2}$. In other words, at high angular frequencies most of the power in the magnetic flux is at high spatial wavenumbers. Given the comparatively shallow depth of the convection only minimal expansion of emergent flux ropes is expected to occur. Consequently, while enhanced activity is present, large-scale inhomogeneities do not occur. Apparently, the transition between "thin" and "thick" (or solar-like) convection zones occurs at about ~ F7 V since it is at this spectral type that the onset of photometric variability occurs [66]. Because of their rapid projected rotation velocities and the lack of large-scale fields, the direct measurement of magnetic field strengths and area coverage have proven very difficult. Moreover, the dominant compact field configuration may account for the rapid rotation of these stars as a class since the lever arm for magnetic braking via a Schatzman-like mechanism [51, 52] is reduced.

6.2. M dwarf stars

The observation of magnetic field-related activity, particularly flare activity, has had a long history that we will not attempt to review here. An early review is given by Mullan [76]. Instead we will focus on a few aspects of dynamo-related properties in these fascinating objects where non-magnetic heating processes are minimized and the contrast between short-wavelength activity and the cool photosphere is maximized.

It had been thought that all M dwarfs later than about ~M5 were dMe flare stars. However, Giampapa and Liebert [77] identified dwarf M stars with spectral types beyond the onset of full interior convection that did not exhibit Hα emission. These stars generally had high proper motions and tended to belong to an older kinematic population. The non-dMe stars could exhibit Hα in absorption, which is an indicator of the presence of chromospheric heating since the Hα line would be weak or not detectable in only a cool photosphere [78]. This fact led to the conclusion that the fractional area coverage of magnetic fields on non-dMe stars must be significant [79]. By the same token, it implied that the distinction between dMe and non-dMe stars could not be due to the filling factor of magnetic regions alone since the chromospheric Hα absorption line could not be changed into an emission line simply by adjusting the filling factor. Thus, intrinsic heating rates in the chromospheres of dMe and non-dMe stars must be different.

Interestingly, the origin of dMe chromospheres may be in downwardly directed coronal X-ray emission [80]. Corroborative evidence on the basis of energy balance arguments for this mechanism is given

in Giampapa *et al* [81] though the question of the origin of the coronal emission remains. The coronal properties of the dwarf M stars are discussed extensively by Giampapa *et al* [82]. The key results are that the coronae of these low mass dwarfs consist of a soft component with solar-like coronal temperatures and a hard component with temperatures ~ 10^7 K. In dMe stars, this high-temperature component dominates the coronal emission and produces the variable X-ray emission observed in these active stars. By contrast, most of the coronal emission measure in dM stars is non-variable and due to the soft component. The coronal structure in these dwarfs is dominated by compact, quiescent loop configurations and an unstable flaring component, which has implications for angular momentum evolution. In particular, the compact loop structure with the implied small lever arm suggests a natural explanation for the observed mass dependence of angular momentum evolution in late-type, main-sequence stars. The dynamo properties of M dwarfs in the context of cycles are discussed in the next section.

7 Frontiers in solar-stellar astrophysics

An imperative of the solar-stellar connection is to obtain the same kind of synoptic information that we acquire for the Sun but, of course, spanning the broader parameter space available to us with stellar observations. In addition to finding a way to continue the pioneering field star studies of the Mt. Wilson HK monitoring program, and the Solar-Stellar Spectrograph synoptic program at Lowell Observatory [83], the next step in the investigation of solar-stellar activity cycles is to extend our efforts to open clusters.

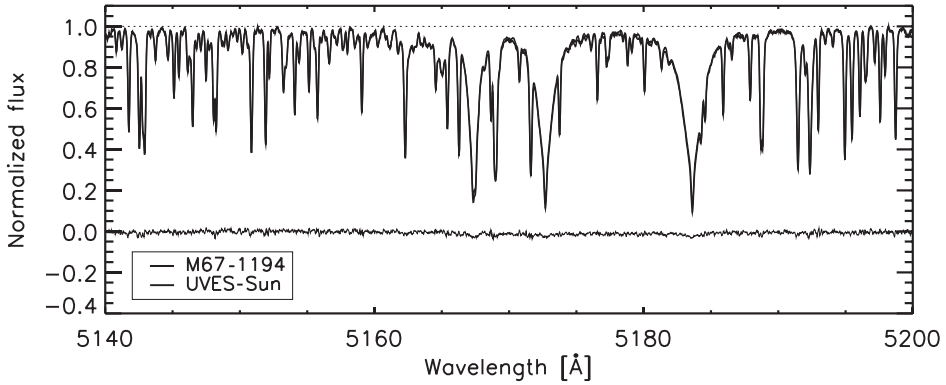

Fig 7. Overlapping spectra in the Mg I*b* triplet region for the Sun and a solar twin in the M67 open cluster (from Ref [84]). The difference spectrum is given below revealing practically negligible residuals.

Synoptic observations of selected open clusters offer a coherent and systematic approach to the study of activity in solar-type stars in populations that are homogeneous in age and chemical abundance. With metallicity and age similar to that of the Sun, the M67 open cluster is a stellar laboratory for the investigation of solar counterparts. In fact, Önehag *et al* [84] investigated a solar twin in M67 with a photospheric spectrum virtually indistinguishable from that of the Sun at their echelle resolutions (Fig 7).

Giampapa *et al* [33] conducted a Ca II H and K survey of the solar-type stars in M67 utilizing the 3.5-m WIYN telescope in conjunction with the Hydra multiobject spectrograph. The principal result is encapsulated in Fig 8 from [33] showing the distribution of an index representing summed Ca II H and K strengths compared to that of the solar cycle from 1976 – 2004. Significant overlap between the Sun and the stellar distribution is apparent along with some departures. About ~75% of the M67 solar-type stars have chromospheric HK indices within the range of the solar cycle, indicating that the Sun is not exceptional or unusual in this regard. However, ~25% of this homogeneous sample exhibit chromospheric H+K strengths that are outside the range of the contemporary solar cycle. These objects are characterized

by quiescent emission below that of the solar minimum (about 17%) or are active with HK indices in excess of solar maximum. Recently, Curtis [85] tentatively suggested that contamination of the HK index from interstellar absorption in the line of sight may lead to an upward revision of the M67 distribution in Fig 8 that could tentatively reduce the overlap with the Sun to ~ 52%. The quantitative impact of the ISM effects still needs to be examined in detail on a per star basis, including a possible spatial variation of interstellar extinction across the cluster taken into account. Nevertheless, the overlap with the Sun would remain substantial though the estimates for the frequency of excursions that may occur in the Sun in excess of solar maximum and how often it could enter into a Maunder minimum-like state would change.

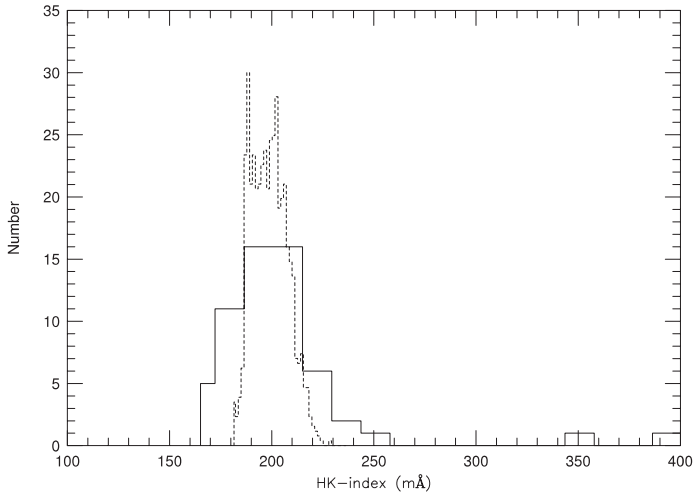

Fig 8. The distribution of an index representing the core strength of the Ca II H and K lines in solar-type stars in M67 (solid line) and the Sun as a star (dashed line) as seen during 1976 – 2004.

In a subsequent study, Reiners and Giampapa [54] utilized high-resolution spectroscopy to measure projected rotation velocities of selected solar-counterparts. With the exception of two interesting objects, only upper limits at the solar rotational velocity of about 2 km s^{-1} were obtained, further confirming the similarity of these objects to the Sun in the context of angular momentum evolution and dynamo generated activity. Since the M67 H&K survey data were obtained over six seasons of observation it is possible to gain some insight on the periods of likely cycles that may be present. Giampapa *et al* [33] did not find evidence for the occurrence of relatively short cycles in any of the sun-like stars observed. However, real variation was detected that, when compared to ~ 6 year sequences within the solar cycle, are suggestive of cycles with periods very similar to that of the Sun, i.e., ~ 10 years. Spectra of a subset of the original M67 sample have only just been obtained at the time of this writing that are contemporaneous with the *K2* satellite campaign, which obtained an ~ 80-day continuous sequence of high precision photometry that included the M67 field. It will be interesting to compare these recent H&K measurements with the results in Giampapa *et al* [33] obtained more than a decade earlier as well as to compare the nature of the photometric variability with the level of H & K emission for each sun-like star.

The next step is to expand the M67 survey to a synoptic study of open clusters spanning a range of evolutionary ages. Accessible clusters include the Pleiades (age ~ 0.1 Gyr), the Hyades (age ~ 0.6 – 1 Gyr), and NGC 752 (age ~ 2 Gyr). Including M67, these clusters form an age sequence that enables a delineation of the evolution of dynamo properties in solar-like stars from about the zero-age main sequence to solar age. Surprisingly, there are not yet published surveys of chromospheric H & K emission in these clusters though

there are Hα observations of members of most of these clusters [e.g., 86]. However, Ca II H and K spectra are in the process of being acquired at the time of this writing and are expected to be forthcoming [85].

7.1 Cycles in M dwarf stars

As discussed in §6, the M dwarf stars span a critical boundary in the context of dynamo models based on the existence of a tachocline since these cool stars become fully convective roughly in the region of ~ M3 – 4 V. If cycles analogous to the solar cycle are a phenomenon unique to shell dynamos then we may not observe cycles in late dwarf M spectral types (but see [87] for a discussion of dynamo action in fully convective M dwarfs).

There are only sparse data on possible cycle variations in M dwarfs though the initial results are tantalizing. Buccino *et al* [88] report the detection of multiple cycles in chromospheric lines and broadband photometry in independent spectroscopic and photometric programs that include the dM3e flare star, AD Leo. At this spectral type, AD Leo is near the fully convective boundary. Buccino *et al* [88] determine the occurrence of an activity cycle in Hα and the Johnson V band with a period of approximately 7 years and a shorter period of 2 years at lower significance. These investigators attribute the longer period to a near-surface dynamo driven by rotational shear while they claim that the shorter cycle originates deep within the convection zone. The relation between the cycle frequencies and the stellar rotation frequency is consistent with the relation found by Saar [43] of $\omega_{cyc} \sim \Omega^{1.1}$.

In an investigation of a long-term data-set obtained for the detection of Doppler variations due to exoplanets in M dwarf stars, Robertson *et al* [89] find that cycles with periods exceeding one year appear for at least 5% of the targets. Specifically, periods were identified in six stars in the range of ~ days to greater than 10 years in addition to long-term trends for seven additional objects. For five objects, periods are in the range 0.73 years to 7.36 years. A critical question is whether the absence of a detectable cycle-like period in the majority of the sample is truly a physical result indicative of the nature of dynamo generation in these cool dwarfs or if it is an artifact of the use of Hα as the activity indicator. In particular, Hα is subject to more stochastic variability [e.g., 90] as a result of flaring and microflaring and may be less preferable than, say, the Ca II resonance lines that are formed lower in the dwarf M chromosphere and therefore more near the surface (photospheric) magnetic flux [15, 91].

A systematic, long-term monitoring program in suitable spectroscopic features and photometric bands of an appropriately selected sample of M dwarfs is urgently needed. Mauas *et al* [92] summarizes results to date of such a program that includes both photometric and spectroscopy observations though the sample size is small. The basic characteristics of a well-constructed stellar sample should include dwarf M stars that span the range from partial to full interior convection, and active flare stars along with more quiescent, non-dMe stars. The latter differentiation essentially segregates the sample by rotation rate as a critical parameter in dynamo field generation. Finally, the utilization of multiple radiative diagnostics in the visible and infrared that are sensitive to magnetic activity and formed at a sequence of temperatures would provide a comprehensive picture of dynamo-related properties in these stars.

7.2 Stellar Magnetic Field Measurements

Thus far we have focused on radiative proxies of magnetic field-related activity because of their accessibility. The direct measurement of magnetic fields in late-type stars has been challenging because of tangled field topologies that yield no net circular polarization or only a residual polarization signal in favorable geometrical circumstances. An advance occurred when Robinson *et al* [93] utilized unpolarized, white-light measurements to directly detect the presence of Zeeman broadening in the wings of magnetically sensitive lines as compared to insensitive (or much less sensitive) lines from the same multiplet. Robinson [94] discusses the formalism for the Fourier deconvolution technique that yields a measure of magnetic field strength and fractional area coverage as interpreted with a schematic representation of the Zeeman triplet

splitting pattern. Saar [95] gives a summary of the advantages, pitfalls and developments in the application of this approach that remains relevant today.

The infrared offers real advantages in stellar magnetic field measurements given that Zeeman splitting is proportional to λ^2 though in practice the gain is proportional to λ since natural line (Doppler) widths increase directly with wavelength. Applications of direct detections of Zeeman broadening in the infrared in stellar and solar magnetic field measurements are given by [96, 97, 98, 99, 100]. The inferred field strengths from these investigations were generally near the gas equipartion value for the surrounding photosphere. In view of this, a recurring hypothesis arose that the primary difference between active and quiet stars was due to the amount of magnetic flux that appeared on the stellar surface. The reader is referred to [3, 4, 101] for comprehensive reviews of stellar magnetic field measurements across the H-R diagram with the exclusion of degenerate objects such as white dwarfs and pulsars. Here we summarize some of the principal techniques and examples of results primarily in the context of parameters relevant to stellar dynamos.

The "white-light" approach described above has been extended with modern spectropolarimetric approaches that are particularly sensitive to the large-scale field and toroidal flux component. An example is the long-term polarimetric monitoring of the solar-type star ξ Boo A (G8 V) by Morgenthaler *et al* [102]. These investigators find that the large-scale field on ξ Boo A is characterized by an axisymmetric component that is dominated by its toroidal component. Interestingly, an earlier study of the presumably fully convective, active dwarf M star, V374 Peg, also reveals a magnetic field structure dominated by a strong axisymmetric component [103] in the presence of only weak differential rotation. Morin *et al* [103] note that this finding is in contrast to dynamo theories that require strong antisolar differential rotation in order to sustain a strong axisymmetric field component while only non-axisymmetric geometries would occur in the presence of weak differential rotation [104, 105]. A more detailed discussion of field topologies in M dwarf stars is given by Gastin *et al* [106]. In addition to global field topologies, the magnetic field properties of starspots are a new area of spectropolarimetric investigation. Afram and Berdyugina [107] discuss the utilization of molecules to infer starspot field characteristics from Stokes V signals.

Doppler imaging relies on high-resolution spectra to detect the distortions in the cores of absorption line profiles as rotation carries thermal inhomogeneities across the line of sight. Pioneered by Vogt and Penrod [108], Doppler imaging is best applied to stars with high projected rotational velocities so that the signature of a cool spot is resolvable in velocity space as its line-of-sight rotational velocity component traverses the absorption core. These objects also probe dynamo properties in the limit of rapid rotation and, generally, thick convection zones. Through the application of inversion techniques, Doppler imaging yields a mapping of cool spots on the stellar surface as a function of phase [109, 110]. The primary targets of Doppler imaging tend to exhibit large polar spots that appear to be long lived, relatively stable structures [see review in Ref 111].

In addition to Zeeman broadening detection and net circular polarization measurements, Zeeman Doppler Imaging (ZDI) is actively utilized for discerning magnetic field properties in rapidly rotating stars. This technique combines Doppler imaging with Zeeman spectropolarimetry to detect rotationally modulated Zeeman components in a magnetically sensitive line. Through this approach the poloidal and toroidal components of the large-scale stellar magnetic field can be deduced to unveil the nature of field topologies in active stars. The broad conclusions thus far from ZDI and other magnetic field studies suggest that stars more massive than 0.5 $M_\odot$ and with Rossby numbers near unity are characterized by a mainly non-axisymmetric poloidal component and a significant toroidal component. In contrast, less massive, active stars produce strong large-scale poloidal and axisymmetric fields [4].

Another accessible spectral feature that is uniquely powerful as a radiative proxy for surface magnetic field regions in the Sun and solar-type stars is the He I triplet line at 1083 nm. This feature (as well as the weaker He I triplet line at 587.6 nm) appears in absorption in active (plage) regions on the Sun

and, by implication, in the magnetic regions on Sun-like stars. The 1083 nm absorption line is not seen, or appears only very weakly, in the quiet solar (or late-type dwarf stellar) photosphere. The 1083 nm line is spatially correlated with significant concentrations of magnetic flux in the photosphere and sites of X-ray emission in the corona but is otherwise only weakly present in the quiet photosphere. Thus, the absorption equivalent width of the 1083 nm line in the integrated spectrum of the Sun or that of a solar-type star can yield direct information on the filling factor of magnetic regions, when properly calibrated by models or through empirical approaches [112].

In a detection of Zeeman broadening in a magnetically sensitive infrared line in the spectrum of the active RS Canum Venaticorum star, λ Andromedae, Giampapa *et al* [96] determined a field strength similar to the photospheric gas equipartition value, based on model photospheres for an object of its estimated gravity and metallicity. Since that time other investigators have carried out similar analyses to find systematic trends in the magnetic properties of (primarily) active stars. Valenti and Johns-Krull [113] summarize these results noting that for G-M dwarfs the measured field strengths cluster around the photospheric gas equipartition value, independent of rotation frequency (Fig 9). Interestingly, the estimated fractional area coverage of magnetic fields increases linearly with rotation frequency, suggesting that the origin of differences in magnetic activity is due primarily to the filling factor of plage-like regions. Examined in more detail, however, there appears to be a demarcation around a rotation period ~ 10 days where average field strengths are less than gas equipartition values while exceeding them for periods less than about 5 days (Fig 9). The pre-main sequence T Tauri stars are an exception with enhanced field strengths more similar to a sunspot and underluminous in X-rays for their field strengths [114].

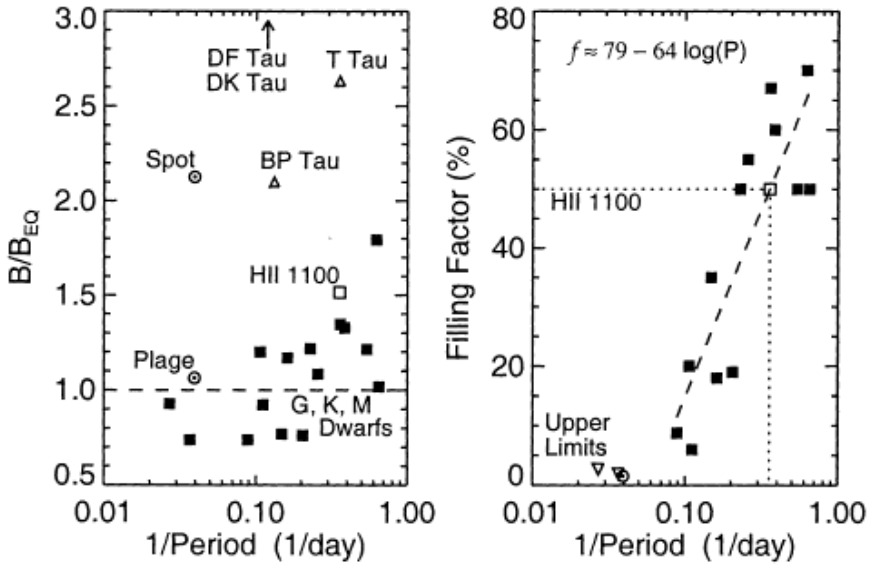

Fig 9. The measured field strength normalized to the photospheric gas equipartition value vs. inverse period (left panel) and filling factor of magnetic fields, also as a function of inverse period (right panel). From Ref [113].

The dwarf M stars merit further discussion in the context of field measurements since it is in this region where dynamo generation may undergo a transition that could be reflected in magnetic field properties. The stored magnetic energy in large-scale configurations (as inferred from Stokes V polarimetry) is twice as large in fully convective M dwarfs than in partially convective dwarf M stars [60, 101]. Nevertheless, in both cases the total magnetic field energy is dominated by small-scale structures.

The next step in this fundamental area of the solar-stellar connection is to obtain (1) long-term polarimetric studies of the cycle modulation of field topologies for F to M dwarfs and (2) extend magnetic field studies to higher sensitivities in order to obtain information on more nearly solar-like stars with solar rotation periods. The latter will be particularly important in order to understand the extent to which solar global topologies are shared among solar-type stars and whether the solar dynamo is somehow unique. An initial observational approach may be found through the analysis of magnetically sensitive lines in the spectrum of the Sun as a star followed by the adaptation of this approach to stellar spectra. However, this may require spectral resolutions in the range of $\lambda/\Delta\lambda \sim 250{,}000 - 300{,}000$ that normally are not available with spectrographs in operation at nighttime facilities today.

7.3 Asteroseismology and the solar-stellar connection

Asteroseismology is the natural extension of the techniques of helioseismology to stars. By enabling the comparison of interior models with experimental results, asteroseismology is the next frontier in stellar astrophysics. Within the solar-stellar connection asteroseismology offers additional approaches to the measurement of parameters relevant to dynamo theory.

In brief review, the *p*-mode oscillations in late-type stars are represented as radial eigenmodes multiplied by a spherical harmonic given by two quantum numbers, *n* and *l*. The radial order *n* is the number of nodes in the eigenfunction between the center and the stellar surface. For solar-type stars, we typically have $n \sim 20$. The angular quantum number *l* is the number of nodal planes that intersect the surface of the star. For observations in integrated light, *l* is small ($l = 0$, 1, 2, or perhaps, 3). Differences in frequency of oscillation of these modes are related to the intrinsic stellar parameters. Frequency separations of the *n*-modes are typically large, and are related to the time for a sound wave to cross the star. Through further consideration of the virial theorem, it can be shown that this travel time is related to the mean density of the star. Thus, the separation of the *n*-modes, known as the "large separation", is easily interpreted in terms of stellar structure and it is relatively more straightforward to observe than the *l* modes.

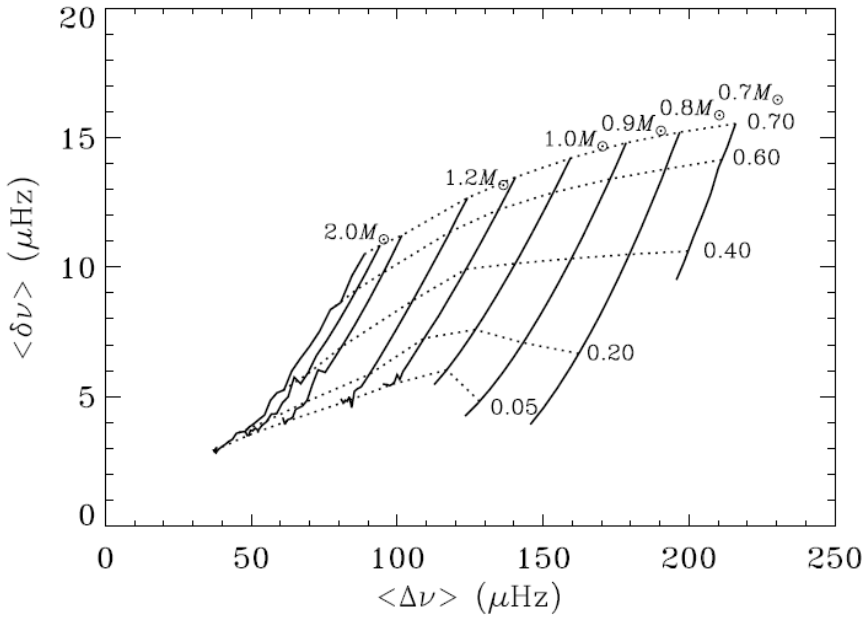

Fig 10. The "asteroseismic H-R diagram" showing the small frequency separation as a function of the large frequency separation along with stellar mass and age. Mass is constant along solid lines; age (parameterized by the central hydrogen abundance) is constant along dotted lines (adapted from Ref 115).

Frequency separations of the *l*-modes are smaller and are related to the radial gradient of the sound speed, particularly in the stellar core. Since these gradients change as nuclear burning alters the molecular weight distribution in and around the core, the so-called "small separation" contains information about the evolutionary state of the star. Measurement of the *l*- and *n*-mode frequency separations can yield good estimates of mass and age when combined with stellar models and other observational parameters. The information content for stars with these frequency separations is summarized in Fig 10 from [115].

Aerts *et al* [116] reviewed the early results from the search for the stellar counterparts of solar-like oscillations. Brown *et al* [117] obtained the first convincing evidence of stellar *p*-mode oscillations similar to that of the Sun for α CMi (Procyon, F5 IV). The first detection of individual frequencies of solar-like oscillations was achieved in 1995 based on high precision time-resolved spectroscopic measurements for the G5 IV star η Boo [118, 119]; however, a confirmation of this detection from independent measurements could not be established, but it was subsequently confirmed by Carrier *et al* [120] and Kjeldsen *et al* [121]. It took another four years before solar-like oscillations were definitely established in Procyon [122]. Solar-like oscillations were found in two more stars: the G2 IV star β Hyi [123] and the near-solar twin α Cen A [124].

The advent of the CoRoT mission followed closely by the *Kepler* mission with its multi-year time series of exquisite photometry in a single ~ 110 square degree field yielded a wealth of new asteroseismic data on stars across the H-R diagram, especially for late-type stars. Chaplin *et al* [125] presented initial results from *Kepler* for three "solar-type" stars with parameters determined from a powerful combination of both seismic and spectroscopic parameters. Consequently, parameters such as effective temperature, mass, radius and surface gravity were determined at high precisions demonstrating that the three objects were slightly more evolved than the Sun [126].

The utility of asteroseismic modeling for the determination of ages for field stars recently has been demonstrated with important implications for gyrochronology [127, 128]. Gyrochronology refers to the determination of stellar ages from rotation periods [63, 129]. The ages based on period-age relations, i.e., gyrochronology, agree for open cluster members at intermediate age (~ 2.5 Gyr). However, an intriguing discrepancy emerges between asteroseismic-determined ages in field stars that are somewhat older than the Sun but with unexpectedly rapid rotation. The origin of this discrepancy may be in the existence of a critical threshold in Rossby number that is related to the nature of the large-scale field configuration that affects rotational braking [55]. The main-sequence progenitor may play a role in the cases of evolved stars. Reiners and Giampapa [54] discuss the role of pre-main sequence disk coupling and decoupling in the existence of relatively rapid rotators at solar age. A long-standing hypothesis often considered in the context of angular momentum conservation is that older stars with rapid rotation may not have exoplanet systems. However, Ceillier *et al* [127] claim that there is no distinction in rotational properties between stellar populations with exoplanets and those for which exoplanets have not been detected.

In addition to fundamental parameters, unusually short periods interpreted as activity cycles have been detected by both CoRoT and *Kepler*, respectively. Fletcher *et al* [130] reported the detection of frequency shifts in an F5 main sequence star that were correlated with a periodic change in a starspot proxy at an estimated period in the range of 120 days – 1 year. The cycle appears to be a fundamental cycle period rather than a secondary cycle period. This work demonstrates that asteroseismology may be a useful tool for the measurement of activity cycles in stars where variations in the amplitude of radiative proxies of magnetic fields are not readily detectable, such as objects where the surface distribution of magnetic regions is fairly uniform throughout a cycle. Perhaps one of the best applications of asteroseismology would be in the identification of true solar counterparts, i.e., stars with a *p* –mode spectrum identical to the Sun as a star. Asteroseismic parameters combined with spectroscopic properties are a powerful approach to determining fundamental stellar properties. The further advancement of this application will require dedicated facilities for multi-year to decadal-long observations.

7.4 Flares and superflaring

The observation of solar and stellar flares is a subject with a long history and an enormous body of literature that merits a review by itself. The study of stellar flares concentrated on cool M dwarf stars where the photospheric contrast is high and flare activity is readily detectable. Recent reviews of solar and stellar flares in the context of the solar-stellar connection are given by [131, 132]. Hilton *et al* [133] give a review of flare activity in cool and ultracool dwarfs while Walkowicz *et al* [134] discuss the statistical properties of white light flares in K – M dwarfs as observed by *Kepler*.

We will focus herein on the recent detection of flaring on solar-type stars at energies that exceed that of the largest solar flares. These events are referred to as "superflares." These exceptionally violent flare outbursts, or 'superflaring' [135], are characterized by energies that exceed the strongest solar flares by one to six orders of magnitude! Notsu *et al* [136] find that superflare frequency increases with increasing rotation rate to a saturation level. Flare energy appears to show a decline with increasing rotation period though with considerable scatter. But it is noteworthy in the context of space weather that superflares have been observed on solar-type stars with solar-like rotation periods [137, 135].

Maehara *et al* [138] discuss the statistical properties of superflare observations at the highest time resolution available with *Kepler* data. Though with scatter in the relation, the total flare energy appears to be proportional to spot group area as inferred from the amplitude of the stellar light curve modulation. The scatter is likely a result of the distribution of inclination angles of the stellar rotation axis, as discussed by Maehara *et al* [138]. This would suggest that superflaring is related to the presence of a relatively larger concentration of surface magnetic flux as compared to the Sun that is then converted into flare energy. More specifically, larger magnetic loop lengths are associated with the greater magnetic flux. Longer loop lengths yield higher volume emission measures for similar plasma densities since $EM \sim nL^3$, where EM is the emission measure, n is the plasma number density and L is loop length. Assuming confinement of the flare plasma in the loop, scaling relations can be derived for the emission measure as a function of magnetic field and flare temperature [139, 140]. A comparison with the data for both solar and stellar flares reveals that the magnetic field strengths associated with the flare region are similar for solar and stellar flares but major stellar flares are hotter with characteristic temperatures $\sim 10^7$ K – 10^8 K while solar flare temperatures are typically less than a few times 10^7 K. Shibata and Yokoyama [141] conclude that stellar flares are hot with emission measures roughly six orders of magnitude larger than that of solar flares because their loop lengths are larger. Finally, we note that Schaefer *et al* [137] suggested that the occurrence of superflaring on ordinary solar-type stars could be due to magnetic reconnection events involving a Jovian-size planet with a magnetosphere in proximity to the star. However, Maehara *et al* [135] found no evidence for transiting planets in the *Kepler* observations of stars exhibiting superflare events.

8 The solar-stellar-exoplanet connection

The study of solar-stellar magnetic phenomena has implications for a broad range of stellar astrophysics that extends from star-disk interactions in the pre-main sequence phase to star-planet interactions. The changing output of solar-type stars—from the time of planet-formation in a given system to the current epoch—provides a critical boundary condition for understanding: (1) the formation and early evolution of planetary atmospheres and (2) climatic variations among more mature planets. Delineating overall energy output, shorter-term transient activity, and longer-term solar-like cyclic activity in sun-like hosts of exo-earth systems yields crucial insight on how frequently earth-like atmospheres are likely to form and survive, and how often exo-earths encounter benign climatic variations.

We know that solar ultraviolet (UV) radiation plays a critical role in the chemistry and dynamics of the earth's atmosphere. Moreover, the UV irradiance of the young Sun may have contributed to the origin

of ozone and free oxygen in the prebiological atmosphere of the young earth [142]. Similarly, the nature of the habitable zones of planetary systems, including the chemical structure and evolution of exo-earth atmospheres, will be impacted by the level and variability of the UV irradiance as its significantly enhanced above the photospheric ultraviolet spectral irradiance by magnetic field-related activity in the host stars over both short and long (cycle-to-evolutionary) time scales.

In the case of the Earth-Sun system, UV radiation from the Sun dissociates molecules, ionizes the neutral atmosphere, and affects many chemical cycles in the terrestrial atmosphere. While the total bolometric luminosity variation of the Sun averaged over a solar cycle is only about 0.1%, the relative variation at solar UV wavelengths is over 10 to 100 times greater depending on wavelength. The solar cycle variability at UV wavelengths longward of 160 nm is 15%; 15% to 70% between 160 nm and 65 nm, and factors of 1.5 to 7 between 65 nm and 1 nm.

The cycle modulation of the solar far ultraviolet (FUV) irradiance as well as previous modeling suggest that we must include the FUV input and its variability in the development of exoplanet atmospheric models. For example, the Canuto *et al* models [142] first demonstrated the viability of producing ozone and free oxygen in an abiotic environment through processes that depend sensitively on UV flux incident on the atmosphere. This result has been affirmed and extended, for example, by Tian *et al* [143] who show that a high UV flux incident on a terrestrial planet in the habitable zone of an M dwarf can result in a large concentration of O_2 through photodissociation of CO_2. The production of ozone follows through the photolysis of O_2—a process that also depends sensitively on the UV radiation field. Obviously, the contribution to the UV irradiance due to activity becomes more important toward cooler stars in the K-M regime, which is the majority stellar type in the Galaxy as reflected in the stellar population in the solar neighborhood. France *et al* [144] further discuss the UV properties of the spectrum of dwarf M stars in the context of exoplanet host star characteristics that can influence exoplanet atmospheric thermal structure and chemistry.

Both O_2 and O_3 are important signatures of life. However, the above results demonstrate that these molecules can emerge through abiotic processes. Therefore, the proper interpretation of future biomarker detection must take into account the contribution to their formation by external influences due, in significant part, to stellar activity. This is especially true for K-M dwarfs where the relative importance of UV emission due to magnetic activity increases as the stellar photospheric contribution declines.

The photochemical and dynamical models for planetary atmospheres are complex and involve a number of molecular species. Stellar UV variability is expected to affect the location of the habitable zone and the formation of complex molecules, including prebiotic molecules that ultimately may provide the foundational pathways to the formation of biogenic molecules. Some of these processes include, in brief (and simplified) synopsis: the photolysis of atmospheric carbon dioxide to produce free oxygen and carbon monoxide ($\lambda \leq 230$ nm) followed by the formation of molecular oxygen; the photolysis of oxygen ($\lambda \leq 200$ nm) then leads to the production of ozone. In parallel with these processes (again in simplified synopsis) is the photolysis of water vapor that, combined with CO (from the photolysis of carbon dioxide) eventually can lead to the production of formaldehyde, H_2CO, which is a key molecule in the formation processes of complex organic molecules.

UV irradiation can disassociate complex molecules unless an ozone layer is preserved. As discussed by [145], energetic protons associated with major flare event entering an exoplanet atmosphere can produce enhancements of mono-nitrogen oxides (NO_x) and species involving the hydroxyl radical (OH_x) that destroy ozone (O_3) through catalytic reactions. In particular, in an investigation of the potential effects of stellar activity on an earth-like atmosphere in the habitable zone of an M dwarf flare star, as discussed by Segura *et al* [145] explored the response of the ozone layer to a powerful flare event characterized by strongly enhanced UV flux and an associated energetic proton flux (Fig 11). In their model calculations, the column density of protective ozone declines catastrophically by a factor ~ 10 in two years after the flare. The ozone

concentration does not recover to its initial column density until about 48 years after the event! Note that this is for a single, major flare event. Since many such flare events occur in active dMe flare stars, the results suggest that the ozone column depth may never recover its initial, steady state value.

The dominant factor affecting the ozone depletion in the Segura *et al* models is the impact of energetic protons on the atmosphere. It is often assumed that this effect is mitigated if the planet has a magnetosphere. However, magnetospheres may not be a guarantee of immunity to stellar activity. For example, another potential effect on the structure and evolution of exoplanet atmospheres, even in the presence of a planetary magnetosphere, is the possibility of atmospheric escape due to stripping by the stellar wind, analogous to the solar wind. A dramatic illustration of how this might occur is seen in an observation recorded by the NASA STEREO-A spacecraft where a CME (coronal mass ejection—an exceptionally violent explosive outburst on the Sun) strips away a piece of the tail of Comet Encke [146].

Vourlidas *et al* [146] attribute the tail disconnection—not to mechanical effects—but to magnetic reconnection events. Oppositely directed fields in the CME interact with (interplanetary) fields entrained in the comet's tail resulting in its separation. With this event in mind, Brain *et al* [147] discuss the possible pathways for atmospheric effects due to the interaction of *exoplanetary* magnetic fields and incident stellar/solar particles, both neutrals and ionized, with entrained fields. On one hand, the planetary field could shield the atmosphere from plasma-related stripping processes resulting in lower loss rates than an unprotected planet. On the other hand, a planetary magnetic field increases the cross-section of the planet to incident plasma, which could lead to higher loss rates. Brain *et al* [147] point to the case of Comet Encke as a proof-of-principle of the latter effect. Stellar activity becomes relevant because the same magnetic field configurations that give rise to activity also modulate the winds and energetic particle fluence emanating from the host star and impacting the exo-earth "magneto-atmospheric" system.

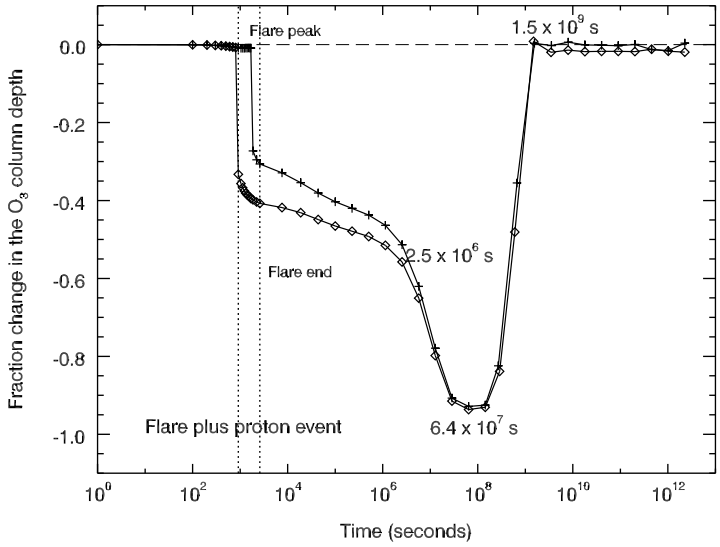

Fig 11. Evolution of the ozone column density relative to the initial conditions prior to the onset of a major stellar flare (from [115]). The results illustrate the impact of enhanced ultraviolet radiation and energetic particle radiation in the form of hard protons as inferred from the characteristics of major flare events observed in a particular M dwarf flare star, AD Leo.

The recent work of Cohen *et al* [148] gives dramatic illustrations of these possible effects in their simulations of the impact of stellar winds in a hypothetical dwarf M—exoplanet system with planets in the

habitable zone. In such cool dwarfs, the habitable zone is in proximity to the central star, or less than about 0.1 – 0.2 AU in the Cohen *et al* models [148]. Though hypothetical, the central star has the properties of a known dMe flare star (EV Lac) and the planetary system configuration is based on *Kepler* discoveries of similar exoplanet system architectures. The models reveal significant interactions between the stellar wind and the exoplanet atmosphere, resulting in substantial Joule heating at the top of the atmosphere. The level of Joule heating is about 0.1% – 0.3% of the total incident stellar irradiation but this can be enhanced by 50% in the time dependent cases considered by Cohen *et al* [148]. Consequently, the potential for planetary atmospheric stripping exists regardless of the presence of an exoplanetary magnetosphere. In fact, the magnetosphere may enhance the effects of upper atmospheric stripping by connecting to the stellar coronal field and effectively guiding energetic particles into the planetary atmosphere. The effects of stellar winds and transient events combined with the enhanced short-wavelength radiation in these magnetically active dwarfs can lead to significant atmospheric erosion for planets in the active M dwarf habitable zone. The next step in this area is to consider the possible pathways for exoplanet atmospheric evolution as the magnetic activity of the host M dwarf declines with age to a more quiescent state characterized by infrequent flare activity and substantially reduced far ultraviolet emittance.

While this discussion of star-planet relationships has focused on M dwarfs, success in coronagraphic imaging and low-resolution spectroscopic observations of true Earth analogs will likely occur first for systems with solar-like hosts. This is because the habitable zone located near ~ 1 AU is sufficiently separated from the host star to make coronagraphic imaging feasible for targets in the solar neighborhood. In an interesting study of earth-like atmospheric evolution in the habitable zones of FGKM stars during a sequence of geological epochs [167], it was found that both the hotter stars and the cool stars yield less biologically damaging radiation following the rise of oxygen concentrations in the exo-earth atmosphere. In the case of the hotter F stars, this is attributed to enhanced ozone shielding as a result of higher ultraviolet environments while for the cooler K – M dwarfs this is ascribed to their lower absolute flux in the UV. The preliminary results of studies of the impacts of irradiation by FGKM hosts on the spectroscopic signatures of biomarkers on earth-like atmospheres in the visible and infrared are not yet in publication at the time of this writing but have been presented in public forums [168]. In a further intriguing diagnostic approach, Berdyugina *et al* [169] examined the potential detection of polarimetric signatures of biomarkers as well as global-scale features such as oceans, clouds and deserts.

While we have focused on the interaction between exoplanets and their stellar hosts, in a novel application the exoplanets themselves can be used to investigate stellar surface magnetic properties in the special case of transiting exoplanet systems. The *Kepler* and CoRoT missions have revealed structure in the bottom of some transit light curves that indicates the presence of underlying thermal inhomogeneities on the stellar surface. The most prominent of these features is seen as a relative brightening of the light curve during the transit, indicating that the exoplanet is passing over a cool spot (Fig 12). In particular, as the transiting planet begins to cross over a spot, it unblocks brighter portions of the stellar photosphere and occults the dimmer starspot, thus producing a relative rise in the photometric light curve [149].

To see in a schematic way how we can infer spot properties, consider the simplified case of a star with a single spot and a transiting exoplanet as seen from Earth. Before the transit the relative flux from the spotted star is described by

$$\frac{F_{stspt}}{F_{star}} = 1 - f_s w, \tag{5}$$

where F_{stspt} ($stspt$ = *"star + spot"*) is the surface flux from the star with a cool starspot in its photosphere, F_{star} is the surface flux of the "immaculate" or unspotted star, f_s is the fractional area coverage or filling factor of the spot on the star, and $w = 1 - F_{spot}/F_{star}$, where F_{spot} is the surface flux of the spot. We see that

the observed signal depends jointly on the relative spot size and the spot contrast. In equation (5) and the following relations we have ignored limb darkening and foreshortening effects.

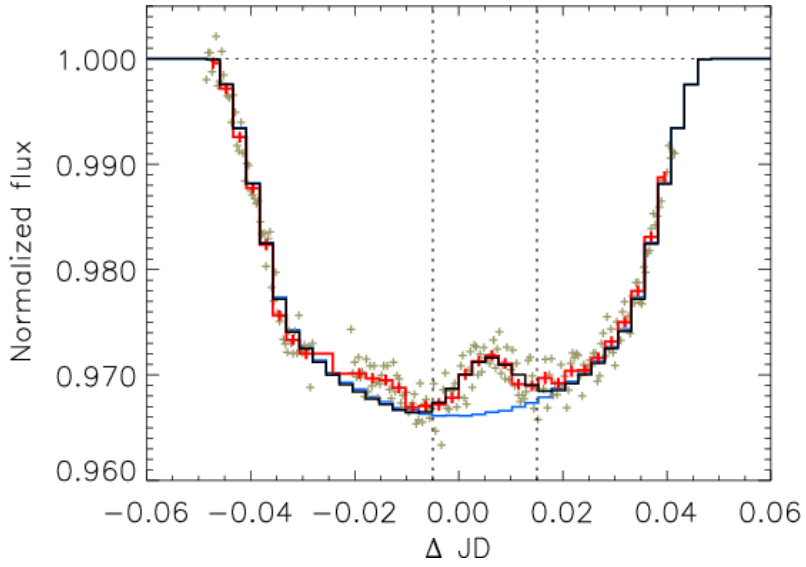

Fig 12. An exoplanet transit of CoRoT-2b from [149]. The relative rise near the center is the characteristic signature of a spot occultation, modeled here as the black curve. The blue line is a transit model for an unspotted star. The smaller bump left of center is due to another spot region not included in their model.

The addition of a transiting exoplanet further reduces the relative flux in Eq (5) by the filling factor of the planet, f_p, or,

$$\frac{F_{sp}}{F_{star}} = \frac{F_{stspt}}{F_{star}} - f_p, \tag{6}$$

where F_{stspt}/F_{star} is given by Eq (5). Here, Eq (6) essentially describes the bottom of the light curve for an exoplanet in transit across a spotted star. In the case where a planet occults a spot that is larger than the projected size of the exoplanet on the star, that is, $f_p < f_s$ (i.e., the transiting exoplanet underfills the spotted region), we have for the normalized flux ("*pos*" = "*planet over spot*")

$$\frac{F_{pos}}{F_{star}} = \frac{F_{stspt}}{F_{star}} f_p\,(1 - w). \tag{7}$$

In the case where the occulting exoplanet overfills the spotted region (i.e., $f_p \geq f_s$) we then have

$$\frac{F_{pos}}{F_{star}} = 1 - f_p. \tag{8}$$

In this case we see only the dark planet against the disk of the star. The relative amplitude of the spot signature during a transit is given by the result of subtracting Eq (6) from either Eq (7) or Eq (8), whichever is applicable. In the case of the former, the result is $\Delta m = f_p\, w_m$ while for the latter it is $\Delta m = f_s\, w_m$, where Δm is the relative amplitude of the "bump" seen at the bottom of the transit light curve in a given photometric band. From these relations it can be shown that, in the first case where the planet underfills the occulted spot, the "color excess" due to the spot is given in two-color photometry by

$$(m_1 - m_2)_{spot} - (m_1 - m_2)_{star} = 2.5 \log \frac{1 - \Delta m_2/f_p}{1 - \Delta m_1/f_p}. \quad (9)$$

In Eq (9), f_p is known and we observe the relative amplitudes of the spot signature during occultation by the exoplanet in two colors represented by m_1 and m_2. In the case where the exoplanet is larger than the occulted spot region we have

$$(m_1 - m_2)_{spot} - (m_1 - m_2)_{star} = 2.5 \log \frac{1 - \Delta m_2/f_s}{1 - \Delta m_1/f_s}. \quad (10)$$

Though the spot filling factor, f_s, in Eq (10) may not be known *a priori,* a very good estimate (or at least a lower limit) can be obtained from the duration of the occultation. We also note that in the case represented by Eq (10) the exoplanet relative size, f_p, is an upper limit to the fractional spot area.

To illustrate in more quantitative terms, we estimate the relative amplitude of the spot signature using PHOENIX model atmospheres to represent the star and the spot, respectively, following Fraine *et al* [150]. Adopting the model atmosphere for $T_{\rm eff}$ = 5000 K, log g = 4.5, corresponding to the bright K1.5 V host star in the transiting system, HD 189733; the $T_{\rm eff}$ = 3500 K, log g = 4.5 model for a spot (giving a spot contrast in temperature of 0.70, which is in the range seen on the Sun); and, using the measured f_p = 2.47% for the transiting large Jupiter, HD 189733b [151], along with two assumed spot filling factors of f_s = 3% and 1.5% [157], respectively, yields the results in Table 1 below for the Sloan *ugriz* bands spanning the visible region and the Johnson *H* band in the near infrared centered at 1.6 μm.

Table1. Model results for a hypothetical spot occultation in HD 189733 (K1.5 V) f_p = 2.47%, f_s = 3% & 1.5%

Sloan + Johnson	u'	g'	r'	i'	z'	H
$\Delta m_{3\%}$	0.0240	0.0234	0.0226	0.0202	0.0182	0.0145
$\Delta m_{1.5\%}$	0.0146	0.0142	0.0137	0.0123	0.0110	0.0088

The color signature of the spot is evident as seen in the decline in relative amplitude from blue to red in the Sloan bands as the spot contrast declines (i.e., the cool spot gets brighter). These changes in brightness and the implied color differences in Eqs (9) and (10) are within the precisions that can be achieved with high precision photometry in the visible and near infrared bands, e.g., utilizing the photometric capabilities available with the SOFIA (Stratospheric Observatory for Infrared Astronomy) airborne observatory [153, 154]. Through high-precision photometry of transiting systems we can learn about the properties of cool spots and possibly magnetically bright regions by modeling of the structure in the transit light curve. We briefly explore the latter possibility in the following.

Suppose we have an exoplanet system with a transiting super-Jupiter and an active host star that exhibits strong chromospheric line emission or, say, strong absorption in the He I λ10830 feature [112]. The observed strength of the λ10830 before (or after) the exoplanet transit is

$$F_{obs} = (1 - f_a)\, F_c + f_a\, F_a \quad (11)$$

where F_{obs} is the observed line strength at 10830 Å, F_c is the local continuum flux, f_a is the fractional area coverage of the active region, and F_a is the intrinsic λ10830 absorption strength in the active region that the planet is traversing. When the exoplanet transits over the active region then the observed line strength in the spatially integrated spectrum of the star is

$$F_{obs} = (1 - f_a)\, F_c + (f_a - f_p) F_a \quad (12)$$

where the notation is as above except that f_p is the relative size of the transiting planet, which is known from prior transit observations. Taking the difference between these two expressions yields

$$F_{obs} = f_p F_a \quad (13)$$

This result makes physical sense and is what we might have expected *a priori*. In particular, the observed change in the observed line strength will depend on the size of the planet and the line strength in the active region. This novel approach thus enables us to determine *intrinsic* active region line strengths that then can be utilized to constrain models of local chromospheric heating in late-type stars.

9 The solar-stellar connection in the new era of astronomy

We have entered a new era in modern astrophysics with the current operation, and advent of major, new observational facilities on the ground and in space. We will discuss the potential of selected facilities for the advancement of the solar-stellar connection.

With its 8.4 m aperture (6.7 m effective aperture) and 3200 megapixel camera, the Large Synoptic Survey Telescope (LSST) will map the entire sky that is accessible to its site in the southern hemisphere 2 – 3 times a week during its 10-year survey lifetime [155]. Characterized by a bright limit for detector saturation in a single 15 second exposure of $r = 15.8$ and a faint limiting magnitude of $r = 24.7$ per visit, the LSST can record brightness variations that may result from cycle modulation of the light curve from late-type stars in multiple Sloan photometric bands, particularly those stars in the solar neighborhood and its representative population (in a Galactic context) of red dwarf stars. The LSST will yield during its first five years of operation, commencing in about 2021, approximately 1,000 data points per star in each of its six filters.

With its sky-survey photometric precision of 5 –10 millimag and 10 year survey duration, LSST will yield data for the characterization of multi-year magnetic activity cycles. Both ground-based, high-precision photometry and recent *Kepler* results confirm cyclic and short-term photometric variations, respectively, in excess of the all-sky LSST precision for chromospheric ages less than ~ 4 Gyr. In the crucial regime of the dwarf M stars where the operative dynamo is expected to undergo a transition as interior structure changes from partially convective to fully convective (near ~ dM4 – dM5), little information on cycles exists. There are preliminary identifications of magnetic activity cycles in four M dwarfs with estimated periods ranging from 1 to 7 years and photometric ranges (min – max) of roughly 40 millimag – 100 millimag. We can therefore expect to compile sufficient statistical information on dwarf M stars that span the range from partial to full convection to see if there are any obvious differences in cycle properties that may arise from this fundamental change in interior structure.

About 10% of the LSST time will be devoted to so-called “deep-drilling” fields where fainter magnitudes and higher precisions are achieved. This, in turn, will enable the detection of cycle modulation of G dwarf stars that have cycle amplitudes that we may expect to see at the age of the Hyades, or somewhat older through the use of co-added exposures. Among the critical goals for LSST to address in this context is the identification of solar-type stars that are in transition to or from grand minima, analogous to the Maunder minimum, along with complementary synoptic spectroscopic data for these objects. The observed brightness variations across the visible band in solar analogs will yield insights on the possible excursion of total solar irradiance (TSI) exhibited by the Sun during the Maunder minimum. This, in turn, will provide important constraints for global climate models.

The LSST will open up the time domain in a way that can contribute to the advancement of astrophysics across the full range of topics, extending from the solar system to cosmology in addition to the solar-stellar connection. The advent of ELTs – Extremely Large Telescopes — similarly will provide new capabilities with the flexibility of spectroscopic as well as imaging instruments combined with an adaptive optics capability. The 24.5-m (equivalent) Giant Magellan Telescope (GMT) [156] and the Thirty Meter Telescope (TMT) [157] are the initial flagship facilities in the new era of ELTs. As one example of the

application of the TMT to the advancement of the Solar-Stellar Connection, M. Giampapa and R. White (Georgia State University) have proposed as a potential Key Project a spectroscopic survey of all northern hemisphere open clusters to a distance of 1000 parsecs, i.e., "The Thousand Parsec Open Cluster Survey." Such a survey would provide fundamental stellar parameters and chromospheric properties of members of nearly ~ 200 different coeval populations, spanning a broad range in age and metallicity. In a solar-stellar context, the Ca II resonance lines and Hα feature, respectively, will be measured as radiative proxies of magnetic fields. These diagnostics will serve as input for models of stellar dynamo evolution that are, in turn, crucial for understanding stellar angular momentum evolution and mass loss, the age-activity relation, and star-planet interactions. With respect to the latter, the open cluster survey will yield candidate hot-Jupiter systems, some of which will transit, yielding a delineation of exoplanet physical properties at a given age and metallicity. In summary, the survey as a Key Project would vastly expand benchmark clusters for model development for open clusters out to 1 kpc.

As an extension of a TMT open cluster effort, it is exciting to examine the feasibility of observing solar-type stars in nearby galaxies beyond the Magellanic Clouds. For example, a G2 dwarf has a V – K color of +1.44 and, at the distance of the Andromeda Galaxy (M31), an apparent K magnitude of 27.9. According to current specifications, the TMT Infrared Multiobject Spectrometer (IRMS), which will enable near diffraction-limited imaging and slit spectroscopy over a 2 arcminute diameter field-of-view at near-infrared wavelengths (0.8 – 2.5 μm), can deliver a signal-to-noise ratio of 22.7 in a 3600 sec integration in dark moon at this magnitude. Through prior work on brighter counterparts in our galaxy, low-to-moderate resolution indices from which metallicity and gravity could be inferred will have been established [e.g., 158]. This kind of program would represent the first practically feasible attempt to identify and carry out a census of the properties of solar-type dwarf stars in an external spiral galaxy with potential implications for understanding the nature of solar-type star formation, including possible exoplanet system formation, in sun-like stars outside our galaxy.

The launch of the *Transiting Exoplanet Survey Satellite* (TESS) satellite in 2017 will mark the start of a two-year survey of the sky for transiting exoplanetary systems in the solar neighborhood [159]. TESS will tile the sky with ~ 27 days of continuous observations at each sector. With its unique High Earth Orbit (HEO), TESS will have an unobstructed view for the acquisition of continuous light curves with two 13.7-day orbits per observation sector. Thus, in addition to transiting exoplanet detection, a wealth of stellar variability data will be obtained at a two-minute cadence that also will enable some asteroseismic analysis for bright solar-type dwarfs and subgiant stars. Similarly, the PLAnetary Transits and Oscillations of stars mission or, PLATO, selected by the European Space Agency for launch in 2024, will obtain high precision asteroseismic data for solar-type stars, including precisely determined parameters of the hosts of discovered exoplanet systems [160]. Asteroseismic determined ages combined with the measurement of rotation periods from the TESS and PLATO missions will yield an independent calibration of the age-rotation relationship to further develop gyrochronology [161, 128].

In addition to the Solar-Stellar Connection, asteroseismology is a tool for other areas of application in astrophysics such as Galactic Archaeology. The *Kepler/K*2 data-set can be culled to identify distant red giants in the halo population utilizing asteroseismic data as a unique signature to distinguish between cool dwarfs and giants [162]. This discriminant, combined with color information, can produce a vetted sample of cool K giants for galactic studies. The K giants are an unbiased population with respect to metallicity and age that, because of their greater luminosity, can be used as distant probes of the halo. As such, the halo red giants can be used to map and date the galactic disk and halo. The PLATO mission will extend these anticipated *K*2 studies. Besides cool stars, missions with an asteroseismic component, such as *K*2, TESS and PLATO, will provide an important complement to the ground-based study of the properties of magnetic hot stars. In particular, investigations of the pulsational characteristics of these objects will yield insight on the

role and impact of non-standard mixing processes in the interiors of hot stars that result in peculiar abundance patterns.

Finally, the Daniel K Inouye Solar Telescope (DKIST) in construction on Haleakala in Maui, Hawaii, will produce unprecedented views of the Sun at fundamental spatial scales when it commences science operations in 2019 [163]. Through this transformative facility, the role of individual magnetic elements in solar dynamics and the origin of magnetic activity can be examined at the highest possible spatial and spectral resolutions. This will enable us to advance our quantitative understanding of how the role of magnetic elements in the aggregate is related to irradiance variations and the generation of mechanical energy that contributes to chromospheric and coronal heating in sun-like stars. In the mid-infrared solar spectrum new spectral diagnostics have been identified in the 3.6 μm – 4.2 μm range that would enable magnetic field measurements simultaneously in the photosphere, chromosphere and corona at sensitivities, in terms of the product $g\lambda$, that are significantly higher than can be attained in the visible [164]. In this way, the empirical relationship between magnetic field properties, and local heating in the chromosphere and corona, can be determined as a critical constraint for models of stellar outer atmospheric heating, among many other applications.

10 Conclusions

Where before it was thought that magnetic field *strength* was the principal discriminant between the so-called 'active' and 'quiet' stars, total magnetic *flux* is widely considered as the origin of the difference between stars that are coronally and chromospherically active, and more quiet stars similar to the Sun. A recurrent theme in the context of systematic trends in dynamo field generation and rotational evolution is the nature of the emergent magnetic topologies. A focus on topology as a distinguishing characteristic for various manifestations of dynamo operation is emerging as a principal research direction.

In rotational evolution and spin-down due to magnetized winds, the relevant critical parameters, whether it is the moment of inertia of the convection zone, the entire star or magnetic topology and the location of the Alvén point, is the dominant factor remains an active area of debate. An extremely challenging but crucially needed measurement is the mass loss rate due to winds (and perhaps transient events) as a function of mass along the main sequence for a well-defined sample.

The tremendous progress of the Solar-Stellar Connection is reflected in the new and deeper questions that research results inspire. Some of these key questions are:

- Can we detect solar-like cycles in the limits of thin and thick convection zones?
- The transition in chromospheric and coronal properties across the transition from partial to full convection appears to be seamless. Therefore, is this transition primarily manifested in changing magnetic field topologies?
- Is the Sun representative of quiescent stars in its dynamo-related characteristics or is it at a transition between "active" and "quiet" stars?
- What is the empirical correlation between field strength and local non-radiative heating in the solar atmosphere?
- Are mass-loss rates similar from F to M dwarfs?
- In rotational decay with time, what is spinning down? Is it the whole star or is it just the outer layers?
- Can the convection zone and radiative interior "decouple" and "recouple" in main-sequence stars on time scales consistent with young, open cluster observations and results from helioseismology?
- Is stellar spin-down a smooth function of time?

- How do we identify stars in a Maunder-minimum state?
- What is the nature of activity-brightness variations for sun-like stars in transition to and from (and during) grand minima?
- How does solar-stellar activity influence the structure and evolution of planetary atmospheres?

The answers to these crucial questions will be facilitated by our willingness to commit the resources needed for the establishment and operation of transformative facilities that will open up new windows on The Solar-Stellar Connection.

Acknowledgements

The author thanks J. C. Hall for a careful reading of the manuscript and his helpful comments and suggestions. The National Solar Observatory is operated by the Association of Universities for Research in Astronomy under a cooperative agreement with the National Science Foundation of the United States.

References

1. Goldberg L, *Publ Astron Soc Pacific*, 97(1985)537-542.
2. Brun A S, García R A, Houdek G, Nancy D, Pinsonneault M, *Space Sci Rev*, 196(2015)303-356.
3. Linsky J L, Schöller M, *Space Sci Rev*, 191(2015)27-76.
4. J -F Donati, Landstreet J D, *Ann Rev Astron Astrophys*, 47(2009)333-370.
5. Hall J C, *Liv Rev Solar Phys*, 5(2008)2.
6. Livingston W C, Wallace L, White O R, Giampapa M S, *Astrophys J*, 657(2007)1137-1149.
7. Livingston W C, White O R, Wallace L, Harvey J, *Mem Soc Astron Italiana*, 81(2010)643-645.
8. Eberhard G, Schwarzschild K, *Astrophys J*, 38(1913)292-295.
9. Skumanich A, Smythe C, Frazier E N, *Astrophys J*, 200(1975)747-764.
10. Auer L, *Astrophys J*, 180(1973)469-472.
11. Auer L, Mihalas D, *Astrophys J*, 158(1969)641-655.
12. Vernazza J E, Avrett E H, Loeser R, *Astrophys J*, 184(1973)605-631.
13. Kelch W L,, Linsky J L, Worden S P, *Astrophys J*, 229(1979)700-712.
14. Baliunas S L, Avrett E H, Hartmann L, Dupree A K, *Astrophys J Lett*, 233(1979)L129-L133.
15. Giampapa M S, Worden S P, Linsky J L, *Astrophys J*, 258(1982)740-760.
16. Linsky J L, *Ann Rev Astron Astrophys*, 18(1980)439-488.
17. Wilson O C, M K Vainu Bappu, *Astrophys J*, 125(1957)661-684.
18. Ayres T R, *Astrophys J*, 228(1979)509-520.
19. Linsky J L, Worden S P, McClintock W, Robertson R M, *Astrophys J Suppl*, 41(1979)47-74.
20. Hudson H S, A*nn Rev Astron Astrophys*, 26(1988)473-507.
21. Wilson O C, *Astrophys J*, 153(1968)221-234.
22. Wilson O C, *Astrophys J*, 226(1978)379-396.
23. Baliunas S L, Donahue R A, Soon W H, Horne J H, Frazer J *et al*, *Astrophys J*, 438(1995)269-287.
24. Baliunas S L, Vaughan A H, *Ann Rev Astron Astrophys*, 23(1985)379-412.
25. Duncan D K, Vaughan A H, Wilson O C, Preston G W, Frazer J, *et al Astrophys J* Suppl, 76(1991)383-430.
26. Noyes R W, Hartman L, Baliunas S L, Duncan D K, Vaughan A H, *Astrophys J*, 279(1984)763-777.
27. Baliunas S L, Nesme-Ribes E, Sokoloff D, Soon W H, *Astrophys J*, 460(1996)848-854.
28. Baliunas S L, Donahue R A, Soon W, Henry G W, in The Tenth Cambridge Workshop on Cool Stars, Stellar Systems and the Sun", eds R A Donahue , J A Bookbinder, *Astron Soc Pacific Conf Ser*, 154(1998)153-172.

29. Fletcher S T, Broomhall A -M, Salabert D, Basu S, Chaplin W J, Elsworth Y, Garcia R A, New R, *Astrophys J Lett*, 718(2010)L19-L22.
30. Baliunas S, Jastrow R, *Nature*, 348(1990)520-523.
31. Wright J T, *Astron J*, 128(2004)1273-1278.
32. Giampapa M S, *Nature*, 348(1990)488-489.
33. Giampapa M S, Hall J C, Radick R R, Baliunas S L, *Astrophys J*, 651(2006)444-461.
34. Hall J C, Lockwood G W, *Astrophys J*, 614(2004)942-946.
35. Choi H, Lee J, Oh S, Kim B, Kim H, Yi Y, *Astrophys J*, 802(2015)67.
36. Skumanich A, *Astrophys J*, 171(1972)565-567.
37. Kraft R P, *Astrophys J*, 150(1967)551-570.
38. Wilson O C, *Astrophys J*, 144(1966)695-708.
39. Pallavicini R, Golub L, Rosner R, Vaiana G S, Ayres T, Linsky J L, *Astrophys J*, 248(1981)279-290.
40. Pizzolato N, Maggio A, Micela G, Sciortino S, Ventura P, *Astron Astrophys*, 397(2003)147-157.
41. Reinhold T, Reiners A, Basri G, *Astron Astrophys*, 560(2013)A4-A22.
42. Giampapa M S, in Comparative magnetic minima: characterizing quiet times in the Sun and stars, (eds) D Webb, C Mandrini, *IAU Symp*, 28(2012)257-267.
43. Saar S H, in The Physics of Sun and Star Spots, (eds) D P Choudhury, K G Strassmeier, *IAU Symp*, 273(2011) 61-67.
44. Saar S H, Brandenburg A, *Astron Nachr*, 323(2002)357-360.
45. Saar S H, Brandenburg A, *Astrophys J*, 524(1999)295-310.
46. Böhm-Vitense E, *Astrophys J*, 657(2007)486-493.
47. Vaughan A H, Preston G W, *Pub Astron Soc Pacific*, 92(1980)385-391.
48. Brandenburg A, Saar S H, Turpin C R, *Astrophys J*, 498(1998)L51-L54.
49. Tobias S M, *Astron Astrophys*, 322(1997)1007-1017.
50. Parker E N, *Res* A*Astron Astrophys*, 14(2014)1-14.
51. Schatzman E, *Annales d'Astrophys*, 25(1962)18-29.
52. Weber E J, Davis L (Jr), *Astrophys J*, 148(1967)217-227.
53. Walter F M, Barry D C, in The Sun in Time, (eds) C P Sonnett, M S Giampapa and M S Matthews, (Univ Arizona Press), 1991, pp 633-657.
54. Reiners A, Giampapa M S *Astrophys J*, 707(2009)852-857.
55. vanSaders J L, Ceillier T, Metcalfe T S, Silva Aguirre V, Pinsonneault M H, García R A, Mathur S, Davies G R, *Nature*, 529(2016)181-184.
56. Stauffer J R, Giampapa M S, Herbst W, Vincent J M, Hartmann L W, Stern R A, *Astrophys J*, 374(1991)142-149.
57. Mestel L, *Astron Nachr*, 305(1984)301-309.
58. Kawaler S D, *Astrophys J*, 333(1988)236-247.
59. Donati J -F, Morin J, Petit P, Delfosse X, Forveille T, Aurière M, Cabanac R, Dintrans B Fares R, Gastine T, Jardine M M, Lignières F, Paletou F, Ramirez Velez J C, Théado S, *Mon Not Royal Astron Soc*, 390(2008)545-560.
60. Reiners A, Basri G, *Astron Astrophys*, 496(2009)787-790.
61. Reiners A, Mohanty S, *Astrophys J*, 746(2012)43-56.
62. Meibom S, Mathieu R D, Stassun K G, *Astrophys J*, 695(2009)679-694.
63. Barnes S A, *Astrophys J*, 586(2003)464-479.
64. Barnes S A, Kim Y-C, *Astrophys J*, 721(2010)675-685.

65. Solanki S K, Krivova N A, Haigh J D, *Ann Rev Astro Astrophys*, 51(2013)311-351.
66. Lockwood G W, Skiff B A, Radick R R, *Astrophys J*, 485(1997)789-811.
67. Radick R R, Lockwood G W, Skiff B A, Baliunas S L, *Astrophys J Suppl*, 118(1998)239-258.
68. Howell S B, Ciardi D R, Giampapa M S, Everett M E, Silva D R, Szkody P, *Astron J*, 151(2016)43-53.
69. Gilliland R L, Chaplin W J, Dunham E W, Argabright V S, Borucki W J, Basri G, Bryson S T, Buzasi D L, Caldwell D A, Elsworth Y P, Jenkins J M, Koch D G, Kolodziejczak J, Miglio A, van Cleve J, Walkowicz L M, Welsh W F, *Astrophys J Suppl*, 197(2011)6-24.
70. Basri G, Walkowicz L M, Reiners A, *Astrophys J*, 769(2013)37-56.
71. Giampapa M S, Astronomy in Focus (2016) in press.
72. Shapiro A I, Solanki S K, Krivova N A, Yeo K L, Schmutz W K, *Astron Astrophys,* 589(2016)A46.
73. Rosner R, *SAO Special Rep*, 389(1980)79-96.
74. Giampapa M S, Rosner R, *Astrophys J Lett*, 286(1984)L19-L22.
75. Schmitt J H M M, Rosner R *Astrophys J*, 265(1983)901-924.
76. Mullan D J, *Irish Astron J*, 12(1976)161-182.
77. Giampapa M S, Liebert J, *Astrophys J*, 305(1986)784-794.
78. Cram L E, Mullan D J, *Astrophys J*, 234(1979)579-587.
79. Giampapa M S, *Astrophys J*, 299(1985)781-784.
80. Cram L E, *Astrophys J*, 253(1982)768-772.
81. Giampapa M S, Golub L, Rosner R, Vaiana G S, Linsky J L, Worden S P, *SAO Special Rep*, 392(1982)73-79.
82. Giampapa M S, Rosner R, Kashyap V, Fleming T A,Schmitt J H M M, Bookbinder J A, *Astrophys J*, 463(1996) 707-725.
83. Hall J C, Lockwood G W, Skiff B A, *Astron J*, 133(2007)862-881.
84. Önehag A, Korn A, Gustafsson B, Stempels E, VandenBerg D A, *Astron Astrophys* 528 (2011) A85-A95.
85. Curtis J L, AAS Meeting, 227 (2016) 105 03
86. Soderblom D R, tauffer J R, Hudon J D, Jones B F, *Astrophys J Suppl*, 85(1993)315-346.
87. Kitchatinov L L, Moss D, Sokoloff D, *Mon Not Royal Astron Soc*, 442(2014)L1-L4.
88. Buccino A P, Petrucci R, Jofré E, Mauas P J D, *Astrophys J Lett*, 781(2014)L9.
89. Robertson P, Endl M, Cochran W D, Dodson-Robinson S E, *Astrophys J*, 764(2013)3.
90. Cutispoto G, Giampapa M S, *Publ Astron Soc Pacific*, 100(1988)1452-1460.
91. Houdebine E R, Junghaus K, Heanue M C, Andrews A D, *Astron Astrophys*, 503(2009)929-944.
92. Mauas P J D, Buccino A, Díaz R, Vieytes M, Petrucci R, Jofre E, Abrevaya X, Luoni M L, Valenzuela P, in Comparative Magnetic Minima: Characterizing quiet times in the Sun and Stars, (eds) D Webb, C Mandrini, *IAU Symp*, 286(2012)317-323.
93. Robinson R D, Worden S P, Harvey J W, *Astrophys J Lett*, 236(1980)L155-L158.
94. Robinson R D (Jr), *Astrophys J*, 239(1980)961-967.
95. Saar S H, in The Impact of Very High S/N Spectroscopy on Stellar Physics, (eds) G Cayrel de Strobel, M Spite, *IAU Symp*, 132(1988)295-300.
96. Giampapa M S, Golub L, Worden S P, *Astrophys J Lett*, 268(1983)L121-L125.
97. Ph Gondoin, Giampapa M S, J A Bookbinder, *Astrophys J*, 297(1985)710-718.
98. Saar S H, Linsky J L *Astrophys J*, 299(1985)L47-L50.
99. Sun W -H, Giampapa M S, Worden S P, *Astrophys J*, 312(1987)930-942.
100. Valenti J A, Marcy G W, Basri G, *Astrophys J*, 439(1995)939-956.
101. Reiners A, *Liv Rev Solar Phys*, 8(2012)1.

102. Moregenthaler A, Petit P, Saar S, Solanki S K, Morin J, Marsden S C, Aurière M, Dintrans B, Fares R, Gastine T, Lanoux J, Lignières F, Paletou F, Ramírez Vélez J C, Théado S, Van Grootel V, *Astron Astrophys*, 540(2012) A138-A152.
103. Morin J, Donati J –F, Petit P, Delfosse X, Forveille T, Albert L, Aurière M, Cabanac R, Dintrans B, Fares R, Gastine T, Jardine M M, Lignières F, Paletou F, Ramirez Velez J C, Théado S, *Mon Not Royal Astron Soc*, 390 (2008)567-581.
104. Dobler W, Stix M, Brandenburg A, *Astrophys J*, 638(2006)336-347.
105. G Chabrier, M Küker, *Astron Astrophys*, 446(2006)1027-1037.
106. Gastine T, Morin J, Duarte L, Reiners A, Christensen U R, Wicht J, *Astron Astrophys*, 549(2013)L5-L8.
107. Afram N, Berdyugina S V, *Astron Astrophys*, 576(2015)A34-A41.
108. Vogt S S, Penrod G D, *Pub Astron Soc Pacific*, 95(1983)565-576.
109. Strassmeier K G, *IAUS*, 273(2011)174-180.
110. Strassmeier K G, *Astron Astrophys Rev*, 17(2009)251-308.
111. Berdyugina S V, *Liv Rev Solar Phys*, 2(2005)8.
112. Andretta V, Giampapa M S, *Astrophys J*, 439 (1995)405-416.
113. Valenti J A, Johns-Krull C, in Magnetic Fields Across the Hertzsprung-Russell Diagram, (eds) G Mathys, S K Solanki, D T Wickramasinghe, *Astron Soc Pacific Conf Ser*, 248(2001)179-188.
114. Johns-Krull C M, *Astrophys J*, 664(2007)975-985.
115. Christensen-Dalsgaard J, *Sol Phys*, 220(2004)137-168.
116. Aerts C, Christensen-Dalsgaard J, Cunha M, Kurtz D W, *Sol Phys*, 251(2008)3-20.
117. Brown T M, Gilliland R L, Noyes R W, Ramsey L W, *Astrophys J*, 368(1991)599-609.
118. Kjeldsen H, Bedding T R, Viskum M, Frandsen S, *Astron J*, 109(1995)13113-1319.
119. Brown T M, Kennelly E J, Korzennik S G, Nisenson P, Noyes R W, *Astrophys J*, 475(1997)322-327.
120. Carrier F, Bouchy F, Eggenberger P, *Astrophys Space Sci*, 284(2003)315-318.
121. Kjeldsen H, Bedding T R, Baldry I K, Bruntt H, Butler R P, Fischer D A, Frandsen S, Gates E L, Grundahl F, Lang K, Marcy G W, Misch A, Vogt S S, *Astron J*, 126(2003)1483-1488.
122. Martíc M, Schmitt J, Lebrun J -C, Barban C, Connes P, Bouchy F, Michel E, Baglin A, Appourchaux T, Bertaux J -L, *Astron Astrophys*, 351(1999)993-1002.
123. Bedding T R, Butler R P, Kjeldsen H, Baldry I K, O'Toole S J, Tinney C G, Marcy G W, Kienzle F, Carrier F, *Astrophys J Lett*, 549(2001)L105-L108.
124. Bouchy F, Carrier F, *Astron Astrophys Astron Astrophys* (*Letter to the Editor*), 374(2001)L5-L8.
125. Chaplin W J, Appourchaux T, Elsworth Y, García R A, Houdek G *et al*, *Astrophys J Lett*, 713(2010)L169-L175.
126. Metcalfe T S, Monteiro M J P F G, Thompson M J, Chaplin W J, Basu S, Bonanno A, Di Mauro, M P, Doğan G, Eggenberger P, Karoff C, Stello D, KASC WG1, *Astron Nachr*, 331(2010)977-980.
127. Ceillier T, van Saders J, García, R A, Metcalfe T S, Creevey O, Mathis S, Mathur S, Pinsonneault M H, Salabert D, Tayar J, *Mon Not Royal Astron Soc*, 456(2016)119-125.
128. Angus R, Aigrain S, Foreman-Mackey D, McQuillan A, *Mon Not Royal Astron Soc*, 450(2015)1787-1798.
129. Mamajek E E, Hillenbr L A, *Astrophys J*, 687(2008)1264-1293.
130. García R A, Mathur S, Salabert D, Ballot J, Régulo C, Metcalfe T S, Baglin A, *Science*, 329 (2010)1032-1032.
131. Fletcher L, Hudson H, Cauzzi G, Getman K V, Giampapa M, Hawley S L, Heinzel P, Johnstone C, Kowalski A F, Osten R A, Pye J, in 6th Cambridge Workshop on Cool Stars, Stellar Systems, and the Sun, (eds) C M. Johns-Krull M K, Browning, A A West, *Astron Soc Pacific Conf Ser*, 448(2011)441-454.
132. Schrijver C J, in 6th Cambridge Workshop on Cool Stars, Stellar Systems, and the Sun, (eds) C M. Johns-Krull M K, Browning, A A West, *Astron Soc Pacific Conf Ser*, 448(2011)231-244.

133. Hilton E J, Kowalski A, Hawley S L, Walkowicz L M, West A A, Magnetic Activity: Flares, Stellar Cycles LSST Science Book, 2009, pp 290-296; arXiv:0912.0201.
134. Walkowicz L M, Basri G, Batalha N, Gilliland R L, Jenkins J, Borucki W J, Koch D, Caldwell D, Dupree A K, Latham D W, Meibom S, Howell S, Brown T M, Bryson S, *Astron J*, 141(2011)50-58.
135. Maehara H, T Shibayama, Notsu S, Notsu Y, Nagao T, Kusaba S, Honda S, Nogami D, Shibata K, *Nature*, 485 (2012)478-481.
136. Notsu Y, T Shibayama, Maehara H, Notsu S, Nagao T, Honda S, Ishii T T, Nogami D, *Astrophys J*, 771(2013) 127.
137. Schaefer B E, King J R, Deliyannis C P, *Astrophys J*, 529(2000)1026-1030.
138. Maehara H, Shibayama T, Notsu Y, Notsu S, Honda S, in Solar and Stellar Flares and Their Effects on Planets, (eds) A G Kosovichev, S L Hawley, P Heinzel, *IAU Symp*, 320(2016)1-6.
139. Yokoyama T, Shibata K, *Astrophys J Lett*, 494(1998)L113-L116.
140. Shibata K, Yokoyama T, *Astrophys J Lett*, 526(1999)L49-L52.
141. Shibata K, Yokoyama T, *Astrophys J*, 577(2002)422-432.
142. Canuto V M, Levine J S, sson T R, Imhoff C L, Giampapa M S, *Nature*, 305(1983)281-286.
143. Tian F, France K, Linsky J L, Mauas P J D, Vieytes M C, *Earth Plen Sci Lett, PSL*, 385(2014)22-27.
144. France K, Froning C S, Linsky J L, Roberge A, Stocke J T, Tian F, Bushinsky R, Désert J –M, Mauas P, Vieytes M, Walkowicz L M, *Astrophys J*, 763(2013)149.
145. Segura A, Walkowicz L M, Meadows V, Kasting J, Hawley S, *Astrobio*, 10(2010)751-771.
146. Vourlidas A, Davis C J, Eyles C J, Crothers S R, Harrison R A, Howard R A, Moses A D, Socker D G, *Astrophys J Lett*, 668(2007)L79-L82.
147. Brain D A, Leblanc F, Luhmann J G, Moore T E,Tian F, in Comparative Climatology of Terrestrial Planets, (eds) S J Mackwell, A A Simon-Miller, J W Harder, M A Bullock, (University of Arizona Press, Tucson), 2013.
148. Cohen O, Drake J J, Glocer A, Garraffo C, Poppenhaeger K, *Astrophys J*, 790(2014)57-69.
149. Wolter U, Schmitt J H M M, Huber K F, Czesla S, Müller H M, Guenther E W, Hatzes A P , *Astron Astrophys*, 504(2009)561-564.
150. Fraine J, Deming D, Benneke B, Knutson H, Jordán A, Espinoza N, Madhusudan N, Wilkins A, Todorov K, Nature, 513(2014)526-529.
151. Pont F, R L Gilliland R L, Moutou C, Charbonneau D, Bouchy F, Brown T M, Mayor, M, Queloz D, Santos N, Udry S, *Astron Astrophys*, 476 (2007) 1347-1355.
152. Winn J N, Holman M J, Henry G W, Roussanova A, Enya K, Yoshii Y, Shporer A, Mazeh T, Johnson J A, Narita N, Suto Y, *Astron J*, 133(2007)1828-1835.
153. Angerhausen D, Mandushev G, Mandell A, Dunham E, Becklin E, Collins P, Hamilton R, Logsdon S E, McElwain M, McLean I, Pfüller E, Savage M, Shenoy S, Vacca W, Cleve J V, Wolf J, *J Astron Teles, Instru, Sys*, 1(2015) 034002.
154. Dunham E W, Bida T A, Collins P L, Mandushev G, Zoonematkermani S, Van Cleve J, Angerhausen D, Mandell A, *et al* Proc SPIE, 9147, in "Ground based and airborne telescopes V", eds S J Ramsay, I S McLean, H Takami, *Proc SPIE*, 9147(2014)91470H.
155. LSST Science Collaboration: Abell P A, Allison J, Anderson S, Andrew J R, Angel J R P *et al*, *LSST Science Book*, Version 2.0 (2009)1-596; arXiv:0912.0201.
156. Johns M, McCarthy P, Raybould K, Bouchez A, Farahani A, Filgueira J, Jacoby G, Shectman S, Sheehan M, in "Ground based and airborne telescopes IV", eds L M Stepp, R Gilmozzi, H J Hall, *Proc SPIE*, 8444(2012) 84441H.
157. Skidmore W, on behalf of the TMT International Science Development Teams, *Res Astron Astrophys*, 15(2015) 1945-2140.
158. Li T, Marshall J L, Lépine S, Williams P, Chavez J, *Astron J*, 148(2014)60-71.

159. Ricker G R, Winn J N, Vanderspek R, Latham D W, Bakos G A *et al*, *J Astron Telesc Instrum, Syst*, 1(2014)014003.

160. Rauer H, Catala C, Aerts C, Appourchaux T, Benz W, Brandeker A *et al*, *Exp Astron*, 38(2014)249-330.

161. Meibom S, Barnes S A, I Platais I, Gilliland R L, D W Latham D W, Mathieu R D, *Nature*, 517(2015)589-591.

162. Miglio A, Chiappini C, Morel T, Barbieri M, Chaplin W J, Girardi L, Montalbán J, Valentini M, Mosser B, Baudin F, Casagrande L, Fossati L, Aguirre V S Baglin A, *Mon Not Royal Astron Soc*, 429(2013)423-428.

163. Keil S L, Rimmele T R, Wagner J, Elmore D, the ATST Team, *ASPC,* 437(2011)319-328.

164. Penn M J, *Liv Rev Solar Phys*, 11(2014)2.

165. Hall J C, Henry G W, Lockwood G W, Skiff B A, Saar S H, *Astrophys J*, 138(2009)312-322.

166. Lockwood G W, Skiff B A, Henry G W, Henry S, Radick R R, Baliunas S L, Donahue R A, Soon W, *Astrophys J Suppl*, 171(2007)260-303.

167. Rugheimer S, Segura A, Kaltenegger L, Sasselov D, *Astrophys J*, 806(2015)137-146.

168. Rugheimer S, Kaltenegger L, Sasselov D, Segura A, *AAS Div for Extreme Solar Systems Abstract*, 3(2015) 500.05.

169. Berdyugina S V, Kuhn J R, Harrington D M, Šantl-Temkiv T, Messersmith E J, *Int J Astrobiology*, 15(2016)45-56.

[*Received*: 1.3.2016; *accepted*: 25.3.2016]